

PHYSICAL MODELING OF RAINFALL-INDUCED LANDSLIDE

A DISSERTATION

SUBMITTED IN PARTIAL FULFILLMENT OF THE REQUIREMENTS
FOR THE AWARD OF DEGREE
OF

MASTER OF TECHNOLOGY

IN

GEOTECHNICAL ENGINEERING

Submitted By

ABHISHEK PRAKASH PASWAN

(Roll No. 2K16/GTE/01)

Under the supervision of

PROF. A.K. SHRIVASTAVA



CIVIL ENGINEERING DEPARTMENT

DELHI TECHNOLOGICAL UNIVERSITY

(Formerly Delhi College Of Engineering)

Bawana Road, Delhi-110042

JULY, 2018

DELHI TECHNOLOGICAL UNIVERSITY
(Formerly Delhi College of Engineering)
Bawana Road, Delhi-110042

CANDIDATE'S DECLARATION

I, Abhishek Prakash Paswan, Roll No. 2K16/GTE/01 of M.Tech. GEOTEHNICAL ENGINEERING, hereby declare that the project Dissertation titled “**PHYSICAL MODELING OF RAINFALL-INDUCED LANDSLIDE**” which is submitted by me to the Department of Civil Engineering, Delhi Technological University, Delhi in partial fulfillment of the requirement for the award of the degree of Master of technology, is original and not copied from any source without proper citation. This work has not been used for the award of any Degree, Diploma Associateship, Fellowship or other similar title or recognition.

Place: Delhi, INDIA

ABHISHEK PRAKASH PASWAN

Date:

DELHI TECHNOLOGICAL UNIVERSITY
(Formerly Delhi College of Engineering)
Bawana Road, Delhi-110042

CERTIFICATE

I hereby certify that the Project Dissertation titled “**PHYSICAL MODELING OF RAINFALL-INDUCED LANDSLIDE**” by **Abhishek Prakash Paswan**, Roll No. **2K16/GTE/01**, Department of Civil Engineering, Delhi in partial fulfillment of the requirement for the award of the degree of Master of Technology, is a record of the project work carried out by the student under my supervision. To the best of my knowledge, this work has not been submitted in parts or full for any Degree or Diploma to this University or elsewhere.

Place: Delhi, India

Date:

Prof. A.K. Shrivastava

SUPERVISOR

Department Of Civil Engineering

Delhi Technological University

Delhi

ACKNOWLEDGEMENT

First, I would like to thank my family, without their love and support over the years; none of this would have been possible. They have always been there for me and I am thankful for everything they have helped me achieve.

I wish to express my deep sense of gratitude and veneration to my supervisor, **Prof. A.K. Shrivastava**, Department of Civil Engineering, Delhi Technological University, Delhi, for his perpetual encouragement, constant guidance, valuable suggestions and continued motivation, which has enabled me to complete this work.

I am also thankful to all the faculty members for their constant guidance and facilities to carry out my work.

Abhishek Prakash Paswan

M.Tech (GTE), DTU

Roll NO. 2K16/GTE/01

ABSTRACT

Rainfall induced landslides are one of the most common and damaging natural hazards in Himalayan region that not only degrade land in hilly areas but additionally causing deaths and destruction on natural slopes (e.g. Hilly areas) and cause tremendous losses. These slope failures usually influence by rain intensities which vary with time that is extremely common in Himachal Pradesh. The intensity and time duration of rainfall over a catchment area decide the property and magnitude of the landslide occurred by the rainfall. Deep slope failure mostly occurred by long duration rain over a catchment area, whereas shallow failure is related to very short-term rain with high intensity. Mostly in shallow slope failure small quantity of soil or debris slides very rapidly. Slope failure which is caused by the rainfall as rain water percolates through the soil layer which in-turn reduces the shear strength of the soil layer.

In Himachal Pradesh a region named Jhakri near NH-5 has recurring slope failure which is broadly affected by the action of rainfall causing significant injury and traffic disruption nearly every year. As NH-5 is only connecting road from outer cities to local areas, stability of slopes on this route have major concern for safe transportation. So this site is selected as a case study for this thesis to study the failure mechanism by the action of rain water, by adopting a physical model. To determine the inherent index properties of soil geotechnical tests has been done in laboratory which affects the stability of existing slope. Further, relation between cumulative rainfall and slope failure pattern has been described.

A physical model is prepared by the theory of semi-similarity which includes the similarity of model size and material used in test and test is performed to examine the failure mechanism occurred by the rainfall with threshold value of rainfall intensity

which is based on the landslide failure occurred at the study area. Numerical Modelling has also been done to analyze the stability of slope using GEO5 software. A rainfall generator is also designed and introduced in test to generate the rainfall of particular depth of rainfall.

The study shows that slope geometry and rainfall intensity are the major affecting parameters which generally introduce the landslide by the action of weathering and percolation of water through the soil pores which leads to the development of lubrication effects between soil particles and hence reduction in shear strength parameter of soil. It also indicates that permeability and density of the soil also play an important role in slope failure mechanism. Relation between cumulative rainfall and slope failure pattern has also been described.

CONTENTS

Title	Page No.
Candidate's Declaration	ii
Certificate	iii
Acknowledgement	iv
Abstract	v
Contents	vii
List of Figures	x
List of Tables	xii
List of Symbols, abbreviations	xiii
CHAPTER 1 INTRODUCTION	1-9
1.1 General	1
1.1.1.Landslides	1
1.1.2.Rainfall	4
1.2 Landslide triggering mechanism related to hydrology	5
1.2.1.Loss of suction	5
1.2.2.Positive pore water pressure	6
1.2.3.Seepage force	7
1.2.4.Seepage erosion	7
1.2.5.Liquefaction	8
1.2.6.Overpressure	8
1.3 Scope	8
1.4 Objective	9

CHAPTER 2	LITERATURE REVIEW	10-15
2.1	Background	10
2.2	Conclusion	15
CHAPTER 3	METHODOLOGY	16-31
3.1	Introduction	16
3.2	Study area	16
3.2.1.	Description of slope	17
3.2.2.	Geotechnical investigation of slope material	18
3.2.3.	Rainfall characteristics	19
3.3	Materials and methods	20
3.3.1	Material similarity and similar condition	20
3.3.2	Laboratory investigation	23
3.3.2.1	Water content	23
3.3.2.2	Particle size distribution	23
3.3.2.3	Specific gravity	25
3.3.2.4	Triaxial test	26
3.3.2.5	Unit weight	27
3.3.2.6	Permeability	29
3.3.3	Experimental set-up	30
3.3.3.1	Experimental platform	31
3.3.3.2	Rainfall generator	31
CHAPTER 4	PHYSICAL MODELLING	33-37
4.1	General	33
4.2	Experimental set-up	34
4.2.1	Frame type box	34
4.2.2	Rainfall generator	35
4.2.2.1	Pump	36
4.2.2.2	Flow regulating valve	36
4.2.2.3	Raindrop nozzle	37

CHAPTER 5	NUMERICAL MODELLING	38-40
5.1	GENERAL	38
5.2	Slope stability analysis	39
5.2.1	Introduction	39
5.2.2	Procedure	40
CHAPTER 6	RESULTS AND DISCUSSION	44-54
6.1	Laboratory results	44
6.2	Physical modeling results	45
6.3	Numerical modeling results	52
6.4	Discussion	54
CHAPTER 7	CONCLUSION	56-57
7.1	Conclusion of results	56
7.2	Future scope of this project	57
REFERENCE		58-61

LIST OF FIGURES

Fig. 1.1: Landslide hazard in Himachal Pradesh	1
Fig. 1.2: Jhakri slope failure along NH-5	3
Fig. 1.3: Average annual Rainfall	4
Fig. 3.1: Location of the study area	17
Fig. 3.2: Jhakri slope scenario a in December 2013 b and c in January 2015 along National Highway-5 near Jhakri town	17
Fig. 3.3: Schematic diagram of slope	18
Fig. 3.4: Monthly precipitation variation	20
Fig. 3.5: Particle size distribution curve for DTU soil	21
Fig. 3.6: Clay	22
Fig. 3.7: Stone and boulders	22
Fig. 3.8: DTU soil	22
Fig. 3.9: Sieve shaker	24
Fig. 3.10: Pycnometer	25
Fig. 3.11: Triaxial test set-up	26
Fig. 3.12: Standard proctor test	28
Fig. 3.13: Schematic diagram of Falling head test set-up	30
Fig 3.14: Schematic diagram of experimental setup	30
Fig. 3.15: Schematic diagram of test model	31
Fig. 3.16: Schematic diagram of rainfall generator	32
Fig. 4.1: Experimental set-up	34
Fig. 4.2: Frame type box with marking on it according to Jhakri slope	34
Fig. 4.3: Frame type model with soil slope	35
Fig. 4.4: Rainfall generator	35
Fig. 4.5: Submersible Pump	36
Fig. 4.6: Flow regulating valve	36
Fig. 4.7: Raindrop sprinkler	37
Fig. 5.1: Co-ordinate range set-up	40
Fig. 5.2: Interface of soil layer	41

Fig. 5.3: Assigning of soil	41
Fig. 5.4: Inputting slip surface	42
Fig. 5.5: Stability analysis of slope by Bishop Method	42
Fig. 6.1: Effect of rainfall at 10 mm depth	45
Fig. 6.2: Effect of rainfall at 20 mm depth	45
Fig. 6.3: Effect of rainfall at 10 mm depth (side view)	46
Fig. 6.4: Effect of rainfall at 10 mm depth (top view)	46
Fig. 6.5: Effect of rainfall at 40mm depth (side view)	47
Fig. 6.6: Effect of rainfall at 40 mm depth (side view)	47
Fig. 6.7: Effect of rainfall at 50mm depth (side view)	48
Fig. 6.8: Effect of rainfall at 50 mm depth (side view)	48
Fig. 6.9: Effect of rainfall at 60mm depth (side view)	49
Fig. 6.10: Effect of rainfall at 60 mm depth (top view)	49
Fig. 6.11: Effect of rainfall at 70mm depth (side view)	50
Fig. 6.12: Effect of rainfall at 70 mm depth (top view)	50
Fig. 6.13: Effect of rainfall at 80mm depth (side view)	51
Fig. 6.14: Effect of rainfall at 80mm depth (top view)	51
Fig. 6.15: Stability analysis of slope by Bishop Method using GEO5 2018 software	52
Fig. 6.16: Stress-strain behavior of soil at 80mm rainfall depth using triaxial test at cell pressure 1.0 kg/cm^2	52
Fig. 6.17: Stress-strain behavior of soil at 80mm rainfall depth using triaxial test at cell pressure 1.0 kg/cm^2	53
Fig. 6.18: Stress-strain behavior of soil at 80mm rainfall depth using triaxial test at cell pressure 1.0 kg/cm^2	53
Fig. 6.19: Stress-strain behavior of soil at 80mm rainfall depth using triaxial test at cell pressure 1.0 kg/cm^2	53

List of tables

Table 1.1: Landslide vulnerable areas in Himachal Pradesh	2
Table 1.2: Major landslide induced by rainfall	3
Table 1.3: Average annual rainfall in mm	4
Table 3.1: Rainfall data of Shimla district	19
Table 3.2: Sieve analysis of DTU soil	21
Table 3.3: Permeability range for different soil	29
Table 5.1: Co-ordinates of interface of soil layers	40
Table 6.1: Soil Properties	44
Table 6.2: Properties of experimental soil obtained by similar material condition	44
Table 6.3: Slope parameters at 80mm rainfall depth	54

List of Abbreviations/symbol

Symbol	Title
KN	Kilo Newton
mm	Millimeter
hr	Hour
Kg	Kilogram
\emptyset	Angle of internal friction
C	Cohesion
E	Modulus of elasticity
OMC	Optimum Moisture Content
MDD	Maximum Dry Density
G	Specific gravity
Γ	Unit Weight
e	Void ratio
w	Water content
k	Permeability
W	Weight of soil
W_s	Weight of solids
W_w	Weight of water
V	Volume of soil
Γ_w	Unit weight of water
W_L	Liquid limit
W_P	Plastic limit
FS	Factor of safety
Γ_d	Dry unit weight
Γ_s	Saturated unit weight
Γ_b	Bulk unit weight

CHAPTER 1

INTRODUCTION

1.1 GENERAL

1.1.1 Landslides

Landslide within the study area is the most common and continual hazard in Himachal Pradesh that causes large risk to life and property. There are number of reoccurring landslide failure occurs every rainy season each year which causes tremendous loss of life and property in the study area due to which life and survival become very difficult for days. The delicate nature of rocks which is the base of formation of hilly areas, along with atmospheric conditions and numerous phylogenesis actions has made the state prone to Landslides. And the rate of landslide increased due to the action of rain water percolation which is the main study part of this report. District wise landslide vulnerability in the State is as follows:

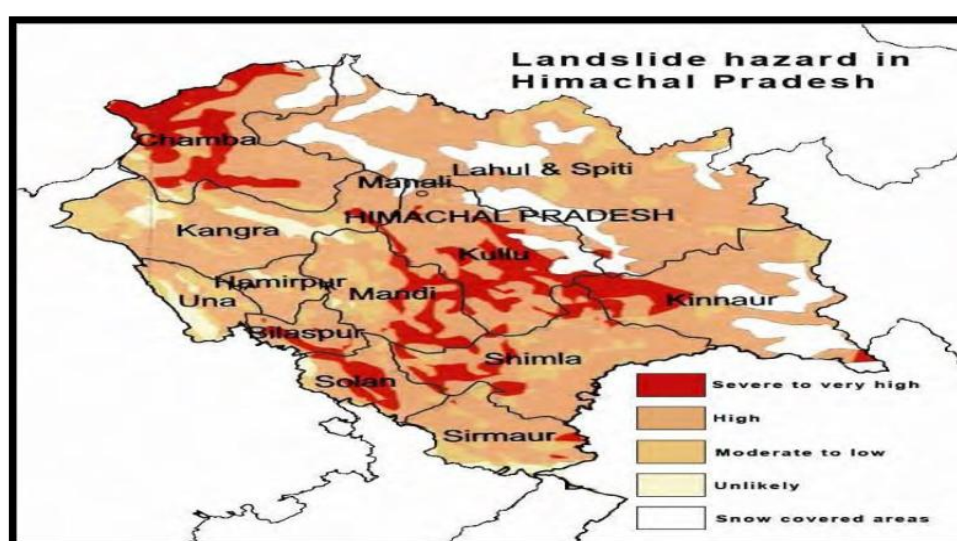


Fig. 1.1: Landslide hazard in Himachal Pradesh
(Source: HPSDMP Himachal Pradesh)
(Link: hpsdma.nic.in/DisasterManagement/HPSDMP.pdf)

Table 1.1 Landslide vulnerable areas in Himachal Pradesh (in square kilometer)
(Source: HPSDMP Himachal Pradesh)
(Link: hpsdma.nic.in/DisasterManagement/HPSDMP.pdf)

District	Severe to high	High	Moderate to low	Unlikely	Total area
Bilaspur	216	842	83	1	1142
Chamba	2120	3829	351	70	6370
Hamirpur	0	851	204	45	1100
Kangra	123	3698	1233	557	5611
Kinnaur	868	4956	498	0	6322
Kullu	1820	3513	65	3	5401
Lahaul & spiti	127	11637	1825	2	13591
Mandi	968	1978	826	98	3870
Shimla	893	3345	767	14	5019
Sirmur	95	1805	614	228	2742
Solan	556	1118	157	79	1910
Una	2	678	517	311	1508

Himalayan slope is more susceptible to landslide failure as compared to landslides occurred around the globe as Himalayan mountain is new fold mountain as compared to others. As these regions are under rapid development in social and economic ways, anthropogenic activities are taking place which is also a main reason for slope failures. As for development part deforestation is taking place which results in loss in shear strength of the soil as we all know the tree roots work as reinforcement with binds the soil particle together which in turn increases the shear strength. As the development is so rapid the designing and material used for construction is also very poor which also affects the stability of slope.

Triggering of landslides is both a natural and anthropogenic phenomena. As in other parts of Himalayas the landslide activity in Himachal Pradesh also varies with

altitude, geology and topography. Various geophysical factors such as steepness of slopes, saturation by heavy rains, melting snow and ice, rock vibrations, excess load from embankments, fills, waste & debris dumps change in water content, frost, change in vegetable cover and toe cutting by rivers and streams are some of the other natural factors influencing the occurrence of landslides. The vulnerability of course has increased many times in the recent past due to various developmental activities. Deforestation, unscientific road construction, terracing, water intensive agricultural practices, and encroachment on steep hill slopes are some of the anthropogenic factors that have contributed towards increased intensity and frequency of landslides. Jhakri, Pangi, Powari, Urni, Sholdan, Nichar, Khadra Dhank, Thangi, Barua are some of the most common landslide that has affected the NH-5 in Satluj valley.

Table 1.2 Major landslide induced by rainfall
(Source: HPSDMP Himachal Pradesh)
(Link: hpsdma.nic.in/DisasterManagement/HPSDMP.pdf)

Name of landslide	Year	Description
Jhakri	1993	Road (NH-5) stretch about half km was completely damaged and slide debris blocked the river Satluj. Traffic restored after two months.



Fig. 1.2: Jhakri slope failure along NH-5
(Source: HPSDMP Himachal Pradesh)
(Link: hpsdma.nic.in/DisasterManagement/HPSDMP.pdf)

1.1.2 Rainfall

As rainfall is the major factor which is accountable in slope failure recurring in nature at every fixed time period, so in my study the effect of rain water percolation is investigated. Average rainfall data of Himachal Pradesh are as follows:

Table 1.3: Average annual rainfall in mm
(Source: Statistical abstract of Himachal Pradesh 2016-17)
(Link: admis.hp.nic.in/himachal/economics/economicsurvey2016-17.htm)

S.No	Districts	2013	2014	2015	2016
1	Bilaspur	1167.4	981.2	1202.0	1048.9
2	Chamba	1308.3	1177.3	1541.9	1059.3
3	Hamirpur	1428.0	1303.7	1481.5	1196.6
4	Kangra	2398.0	1522.3	1996.3	1602.5
5	Kinnaur	1055.0	432.2	710.1	375.5
6	Kullu	1286.4	1191.6	1253.4	1009
7	Lahaul-Spiti	507.9	550.9	825.3	392
8	Mandi	1616.0	1625.1	1524.4	1393.3
9	Shimla	1032.0	1076.7	1088.6	948.2
10	Sirmaur	1807.6	1356.6	1186.8	1028.3
11	Solan	1236.9	1344.2	1382.2	1191.3
12	Una	1455.1	1243.2	1622.0	1034.9

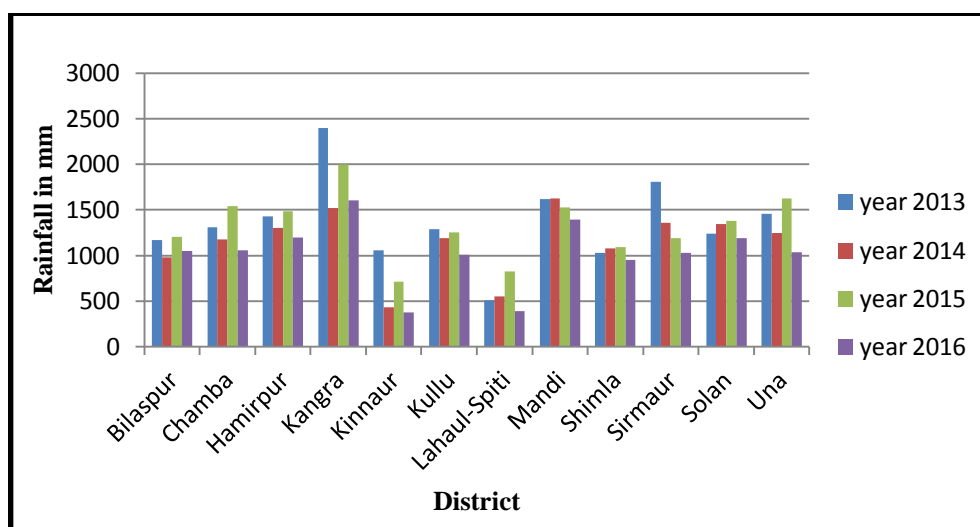


Fig. 1.3: Average annual rainfall

By analyzing the frequency of landslide in monsoonal season and in winter season the result point out that most of the landslides takes place in monsoonal season by the action of heavy rainfall. Rainfall usually triggers slope failures. It acts as a supporting agent for the landslide occurrences. Rainfall triggers the landslides, plays its part and acts as an immediate disturbing agent. Such a failure might have developed increasingly, in the course of propagation of a continual slip surface, strain-softening, weathering and general decrease of shear strength.

The rain water is main cause for destabilization of the earth material on various slopes. Water is directly and indirectly concerned with the occurrences of landslides. The saturation of soil on steep slopes caused by long duration heavy rainfall is responsible for the occurrences of landslides within the Shimla district. Because the soil on the surface becomes saturated, the water makes its approach right down to the lower layers. With excessive rainfall deep percolation takes place between the rock and soil layer which increasingly accumulated and creates the fluid zone near the surface. Which in-turn reduces the shear strength and leads to landslide. Also the sudden and extreme rainfall increases the surface runoff. Thus, removal of vegetation cover and erosion of soil layer of slopes takes place making the slopes more susceptible for landslide.

1.2 LANDSLIDE TRIGGERING MECHANISMS RELATED TO HYDROGEOLOGY

The triggering mechanism describes the physical, chemical and mechanical function of the triggering process that is connected with the loss of strength of the soil. Water influences the stability of slopes in many ways like decreasing suction, positive pore water pressure, and seepage forces reduce the shear strength of soil. The mechanisms are as follows:

1.2.1 Loss of suction

Additional water content leads to decreasing soil suction and thus to decreasing apparent cohesion. A reduction of the suction in unsaturated or partly saturated soil may be sufficient to trigger shallow landslides even if the soil is not completely saturated

according to Equation 1.1; decreasing suction decreases the soil's effective stress. Thus the shear strength is reduced, which destabilizes the slope. The additional weight of water has an extra destabilizing effect on the soil. The moisture content of the soil may remain below saturation if the rainfall infiltration rate is below the hydraulic conductivity. When the percolating wetting front reaches a critical depth in the soil, the slope may become unstable. This depth depends on the cohesion and the slope angle.

$$\tau = C + \sigma_n \tan \varphi \quad (1.1)$$

1.2.2 Positive pore water pressure

A rising groundwater table ("bottom up" saturation) within the saturated zone leads to a gradual growth of pore water pressure in the soil (Iverson et al., 1997). This process is frequently observed during heavy rainfall. As seen in Equation 1.2, an increase in the pore water pressure decreases the effective stresses in the soil (the total stress remains constant under drained conditions). This reduces the shear strength and destabilizes the slope. All types of soil are affected and the response time depends on the permeability of the soil: More permeable soil underlies more rapid changes. It has been shown that also in clayey soil pore water pressure can change rapidly due to secondary permeability as cracks, pressures, lenses of more permeable material (Rogers and Selby, 1980; Duncan and Wright, 2005). A rising positive water pressure can lead to the failure of slopes. Especially deeper landslides (5 m - 20 m deep) are triggered by raising groundwater level and thus positive pore water pressure on the slip surface.

$$\sigma' = \sigma - u \quad (1.2)$$

Cracks formed due to landslide activity or desiccation may be an additional destabilizing element. Hydrostatic pressure can build up in cracks. This additionally loads the soil within the slope and thus destabilizes it.

Saturation of the soil may also occur "top down". Prolonged rainfall with intensity less than or greater than k can lead to vertical downwards steady state infiltration without development of positive pore water pressure even if saturation is

reached. This is because the downward gradient $i = \frac{dh}{dz}$ is assumed to be equal to -1 what implies zero pore water pressure and the downward flux q equals the saturated hydraulic conductivity (k). A saturated zone develops in the top soil and propagates downwards. Iverson et al. (1997) described a mechanism that after a first rainfall event, the soil can remain tension saturated and a subsequent high intensity rainfall can lead to an instantaneous rise in pore water pressure.

1.2.3 Seepage force

Seepage is the water flow through the soil that occurs when parts of the soil are saturated and when the hydraulic gradient is not equal zero. Seepage has basically two effects on the soil strength of the soil, Seepage force and seepage erosion. The seepage force acts on the volume of the soil mass. The viscous drag of water flowing through the soil mass imposes pressure acting on the soil particles in the direction of flow. Thus seepage leads to an additional increase (or decrease) in the pore water pressure what affects the shear strength of the soil. Depending on the direction of the seepage, this fluid pressure may act against the restraining forces and decreases the factor of safety.

1.2.4 Seepage erosion

Seepage erosion (also named inner or internal erosion) is the dragging effect induced by seeping water in granular material (Lourenco et al., 2006). Water that seeps in the soil can lead to a mechanical displacement of soil particles through the soil matrix or to regressive erosion and the formation of pipes. Pipes are preferential flow paths which have a higher permeability than the surrounding material. These processes loosen the soil. Seepage erosion is more efficient in sandy soils where the fine-grained components are washed out. Silt and clay-size fraction of the soil are deposited, eroded, re-deposited within the flow network. This can continually change the permeability and flow path within the slope (Harp et al., 1990). Piping can reduce the contact between grains. This decreases the cohesion and the shear strength can decrease even though the pore water pressure does not rise. This process is particularly active at locations with high permeability and thus high flow velocity. It is not possible to calculate the effect of seepage erosion as it strongly depends on the local characteristics of the soil.

1.2.5 Liquefaction

When a saturated soil completely loses the strength, it collapses entirely and behaves like a fluid because high pore water pressure cannot be relieved. This failure mechanism is called static liquefaction. Liquefaction occurs in both, coarse grained material (silty-clayey sand or gravel) with low plasticity and fine-grained high plastic material. Poorly sorted, loosely compacted, or cohesion-less soils are especially sensitive to liquefaction. Overpressure, upward seepage and strong inner erosion favours liquefaction. If the vertical component of the seepage force is equal or greater than the saturated weight of the cohesion less soil, the effective stresses between the particles becomes zero and thus the frictional strength as well (Iverson and Major, 1986; Budhu and Gobin, 1996; Ghiassian and Ghareh, 2008). Cohesive soil will only liquefy if the cohesive bounds are broken, for example due to earthquake or landslide (dynamic liquefaction). Dynamic liquefaction may be caused when the porosity of the soil is reduced during failure. A reduced porosity leads to an increase of pore water pressure. The porosity may either be reduced due to contraction of the soil mass or if the soil particles dilate.

1.2.6 Overpressure

Overpressure (also named up-thrust pressure, buoyancy forces, uplift) acting on the slip surface from below a landslide builds up if the hydraulic potential in the aquifer below the landslide is higher than in the landslide. This may happen if the permeability of the landslide is smaller than the permeability of the geological unit below the landslide. If an aquifer is limited on the upper boundary by a low permeable or impermeable horizon, it is named semi-confined or confined, respectively. If the hydraulic potential is higher than the ground surface, it is an artesian aquifer. overpressure from below the landslide can act as a trigger mechanism (Rogers and Selby, 1980; Mikos et al., 2004) and may favor upward seepage and liquefaction.

1.3 SCOPE

As rainfall induced landslides is dangerous hazard which has the foremost chances of occurring in each and every monsoonal season which cause tremendous risk to loss

of life and property in-turn affect the social and the economic features and as the developments and urbanization occurring with a high rate in hilly areas like Shimla district as it is also a place for tourism it is most necessary to analyze the causes and mechanism of slope failure so that strengthening of slopes can be done to prevent the slope failure. The study also leads to the installation of early warning system so that the loss can be minimized.

So the study will help in deciding the threshold rainfall for the landslide and practical advice for prevention, monitoring, early warning and control of hazardous landslides which triggered by rain.

1.4 OBJECTIVE

- To study the slope failure mechanism of JHAKRI slope in Shimla, Himachal Pradesh by physical modelling.
- To design a rainfall generator to control the flow of water for generating the desired rainfall intensity with known discharge to introduce desired rainfall depth on the slope.
- To prepare a physical model of slope in laboratory and study its behaviour under rainfall.
- To compare and analyse the stability of slope by Numerical modelling of slope using GEO5 software.

CHAPTER 2

LITERATURE REVIEW

2.1 BACKGROUND

Rainfall induced slope failures occur frequently all over world during rainy season. These types of slope failures have become one of the most dangerous natural hazards worldwide, usually causing economic losses and sometimes even fatalities. These failures commonly occur in natural slopes, particularly residual slopes.

Considerable research has been conducted on the behavior of rainfall induced landslides to study the rainfall induced landslides and failure mechanism of slope. The available body of literature extends over several decades and is rapidly growing. As such, it cannot be adequately summarized in a brief chapter. Instead, a overview of major references is provided here along with useful citations to previous works that contain detailed reviews of related literature.

Li1 et al. (2016) studied slope failure mechanism by adopting a model test on rainfall-induced loess–mudstone interfacial landslides in Qingshuihe, China. In this paper a semi-similar material physical model test was conducted to investigate the start-up conditions and sliding mechanism of rainfall-induced loess- mudstone interfacial landslides based on the landslides occur in China. The loess strata were taken from the site. The mudstone was simulated by similar materials in the test. Therefore, it is named as semi-similar material landslide physical model. Its physical and mechanical properties were tested and analyzed before physical model test was done. The hydrometer analysis method was adopted to test grain-size distribution of soil. The

compaction test, permeability test, triaxial test are done to analyze the properties of soil. The testing equipments of a self-designed frame-type landslide model were adopted, which were composed of experimental platform system, artificial rainfall system, and data collection system. In the test, the overlying loess strata were sampled from in situ while the underlying mudstone strata were used by similar materials.

The results of semi-similar material test indicate that it is an effective method to monitor the pore water infiltration process in the test. The sliding mechanism of interfacial landslide and its influence factors were studied in this study. The results of this study shows:

- The influence of rainfall time intervals on interfacial landslide
- The influence of rock at the back of slope on interfacial landslide
- The influence of overlying loess thickness on interfacial landslide
- The influence of slope gradient on interfacial landslide
- Sliding process of interfacial landslide

There are limitations existing in this study as the geometric size of landslide prototype is relatively large while the size of the indoor model is limited in terms of the testing feasibility. However, it provides a scientific preventive and practical guidance for the prevention, monitoring, early warning and control of geologic hazards of rainfall-induced loess–mudstone interfacial landslide.

Yang et al. (2012) has done their Investigation of rainfall-induced Shallow landslides on the north-eastern rim of Aso caldera, Japan, in July 2012. As the area is affected with heavy rainfall which usually triggers the slope failure. This heavy rainfall triggered many shallow landslides, especially on the north-eastern rim of Aso caldera, leading to significant loss of life and damage to many villages. one landslide site at Ichinomiya (Kumamoto Prefecture) was selected for detailed study. Field and laboratory investigations were conducted to identify the initiation mechanism of the shallow landslides during heavy rainfall.

The thickness of the soil layer was determined using portable dynamic cone penetration tests. The soils became thinner (about 1 m) from the upper to the lower slope. In-situ infiltration tests indicate that hydraulic conductivity of this thin soil layer is low. During heavy rainfall events, most rainfalls will transform into surface runoff instead of infiltration. The results of consolidated-undrained triaxial compression tests show that the effective friction angle and cohesion of the soil are 36.9° and 6.3 kPa, respectively. Soil behavior in response to increase in pore-water pressure was evaluated using a pore-water pressure controlled triaxial test.

The results indicate that the steep slopes on the north-eastern rim of Aso caldera will remain stable under normal rainfall conditions, due to the high shear strength of the soil. The probable initiation mechanism for the shallow landslides on the north-eastern rim of Aso caldera suggests that the initial failure process begins with toe erosion caused by surface runoff during heavy rainfall. Due to the loss of the resistance force at the toe of slope, the slope will reach a critical condition when pore-water pressure in the slope also increases.

Kumar et al. (2017) has done their research on Geotechnical characterization and analysis of rainfall—induced 2009 landslide at Marappalam area of Nilgiris district, Tamil Nadu state, India. Landslide is one of the major natural hazards at Nilgiris in which debris slide is the most common type triggered by heavy intense rainfall (Seshagiri et al. 1982). Since the Nilgiris district is located in the tropical zone, it receives rainfall during both southwest (June to September) and northeast (October to December) monsoons (Chandrasekaran et al. 2013).

In this study field investigation comprises topographical survey, borehole investigation, and geophysical investigation. Topographical survey has been performed to establish the geometry of Marappalam slope such as slope angle, elevation, run-out distance, and width of the landslide. Borehole and geophysical investigations were carried out to identify the properties of soil and rock.

Laboratory tests were performed on soil and rock samples collected from the boreholes and soil samples from test pits as per relevant American Society for Testing

and Materials (ASTM) standards. The tests were conducted to identify index and engineering properties. The laboratory tests on soil comprised specific gravity test, wet sieve analysis, mechanical sieve analysis, hydrometer analysis, Atterberg limits tests [liquid limit (W_L) and plastic limit (W_P)], and hydraulic conductivity test. Based on index properties test, soil samples were classified as per Unified Soil Classification System (USCS). Uniaxial compressive strength test, tensile strength test (Brazilian split-tension test), and point load index strength test were performed on rock core samples. Residual shear strength parameters were identified using repeated direct shear test. Mineral compositions of soil and rock were identified using x-ray diffraction analysis. Scanning electron microscopic analysis was performed to identify the micro fabric nature of soils.

Numerical analysis has been done using LS-RAPID. It is a strength reduction technique-based integrated landslide simulation model that has been developed to assess the initiation and motion of landslides triggered by rainfalls, earthquakes, or a combination of both.

The study concludes that the landslide occurred due to a very high amount of 5-day antecedent rainfall and very high magnitude of daily rainfall. Considering the landslides occurred in Marappalam region and rainfall threshold analysis, the optimum level of rainfall to trigger landslides in Marappalam region is 225 mm of daily rainfall and 110 mm of 5-day antecedent rainfall. During rainfall, water infiltrates into the top soil of loose to medium dense layers and charges down the slope at the interface of soil and impermeable rock layer. This leads to the development of positive pore water pressure and subsequent decrease in the matric suction which in turn reduces the shear resistance of the soil and triggers landslides in Marappalam.

Hence, the slope failure can be prevented by lowering the ground water level by adopting preventive measures such as subsurface horizontal drains made of perforated pipes wrapped with geotextiles. In addition, internal slope reinforcement technique such as slope stabilizing piles can be installed to strengthen the sliding mass above the failure surface by placing the passive piles embedded into stable layer. However, the effectiveness of the above preventive measures requires a detailed study for Marappalam slope.

Luo et al. (2015) has done their research on rainfall-induced shallow Landslides by considering a physical modelling. In this paper, a physical model considered the effect of overland water flow on rainfall-induced shallow landslides is derived and applied to predict the landslides. The slope stability model is developed by considering the depth of overland water flow in infinite slope stability theory. Hill slope hydrology is modelled by coupling the overland uniform water flow equation with Rosso's seepage flow equation. And then, the model is used to assess the slope stability in Dujiangyan of China, and the results is compare with Rosso's model.

The model used is simple, but has the capability of taking into account the effect of overland water flow in the triggering mechanism of shallow landslide. The results of case study show that the overland water flow can make an obvious effect on shallow landslides, so it is quite important to consider the overland water flow in shallow landslide hazard assessment.

Dahal et al. (2008) has done their investigation on failure characteristics of rainfall-induced shallow landslides in granitic terrains of Shikoku Island of Japan. This paper deals with the synoptic descriptions of failures that occurred in the granitic terrain of northeast Shikoku Island, Japan, along with rainfall and failure relationships during the typhoon. The study shows that:

- Typhoon-brought rainfall-induced landslides in the granitic terrain of northeast Shikoku, Japan, in general, can be categorized as shallow, translational slides having failure depth less than 1.5 m. Many slides were subjected to flow down to the slope after sliding.
- The landslides were initiated when the sandy residual soils of the granitic terrains (masa) were 40–100% saturated, depending on the slope angles and vertical depth of the soil. It was also understood that extensive failure occurred in masa soil of Japan during typhoon. Rainfalls, because of a high rate of infiltration and high intensity of rainfall.”

- Temporal rainfall intensity and duration values responsible for failures and calculated from total rainfall events.

2.2 CONCLUSION

Findings suggest that slopes with different soil properties, particularly hydraulic properties have different response to rainfall events. The amount of rainwater infiltration essentially governs the pore water pressure generated in a slope, which in turn controls slope failure. Therefore, the relation between rainfall intensity and soil hydraulic properties should be considered in the analysis of slope stability. It is widely accepted that prolonged rainfall is the main trigger for slope failure during monsoonal season. Slope failure mechanisms are governed by various controlling factors and failure occurs along the weakest paths in the slopes or more specifically the path where the shear stress exceeds the shear strength. These paths may vary in their shapes and constitution, depending on the characteristics of the soil slopes.

Rain water falling on the slope may be partly transferred to runoff rather than completely infiltrating the slope, which introduce weathering action in slope which is also leads to slope failure.

CHAPTER 3

METHODOLOGY

3.1 INTRODUCTION

This chapter describes the materials and methodologies used in this research to ensure the achievement of the study objectives. Region with natural slope failure induced by rainfall is used as the main site for study. Rainfall data from closest station to the study areas is considered in the analysis. The slope dimensions, material properties are taken from a research paper and then material simulation is done by performing grain size distribution to meet the inherent soil property of parent material of slope. Laboratory test is conducted to determine the soil properties required in the analysis.

3.2 STUDY AREA

My study location is on NH-5 (Hindustan-Tibet-Highway) which is also a connecting corridor to other areas of Shimla which is in Jhakri town in Shimla district of Himachal Pradesh, India (Fig. 3.1), which is situated near Sutluj River that is the rainfall catchment basin of the study area. Jhakri area in Shimla district is most vulnerable zone for landslide along the NH-5 triggered by rainfall (Singh et al. 2017).

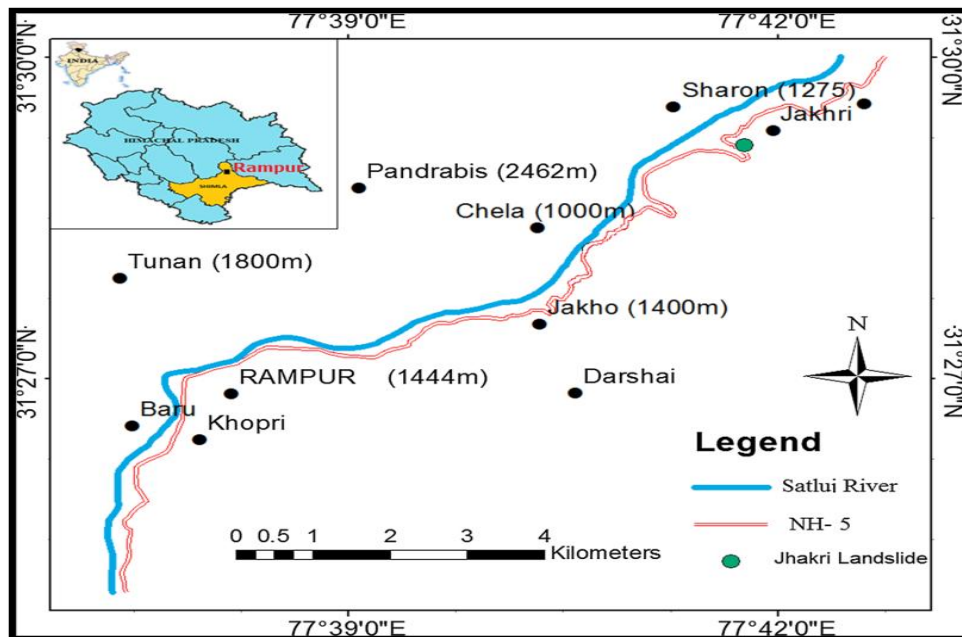


Fig. 3.1: Location of the study area
(Source: Singh et al. 2017)

3.2.1 Description of slope

The studied slope is near the Jhakri town in Shimla district. A tributary of river Satluj. One of the two failed portion of the existing slope which is in southern direction has been studied in present work. In northern side slope has 24–27 m of height with slope angle of 56° and in southern side slope has height of 55.3 m with a slope angle of 35° has been observed.



Fig. 3.2: Jhakri slope scenario; (a) in December 2013, (b) and (c) in January 2015
along National Highway-5 near Jhakri town
(Source: Singh et al. 2017)

The slope contains loose materials deposits composing highly weathered rock particles. The soil material is non-uniform in grain size containing various size of rock and stones. The slope dimensions of southern side are as follows (Singh et al. 2017):

- 1) Slope angle = 35°
- 2) Slope height = 31.7 m
- 3) Base of slope = 45.3 m
- 4) Length of slope = 55.3 m
- 5) Width = 57 m
- 6) Length of crest = 35.7 m
- 7) Length of toe = 16 m
- 8) Height of toe = 4.5 m

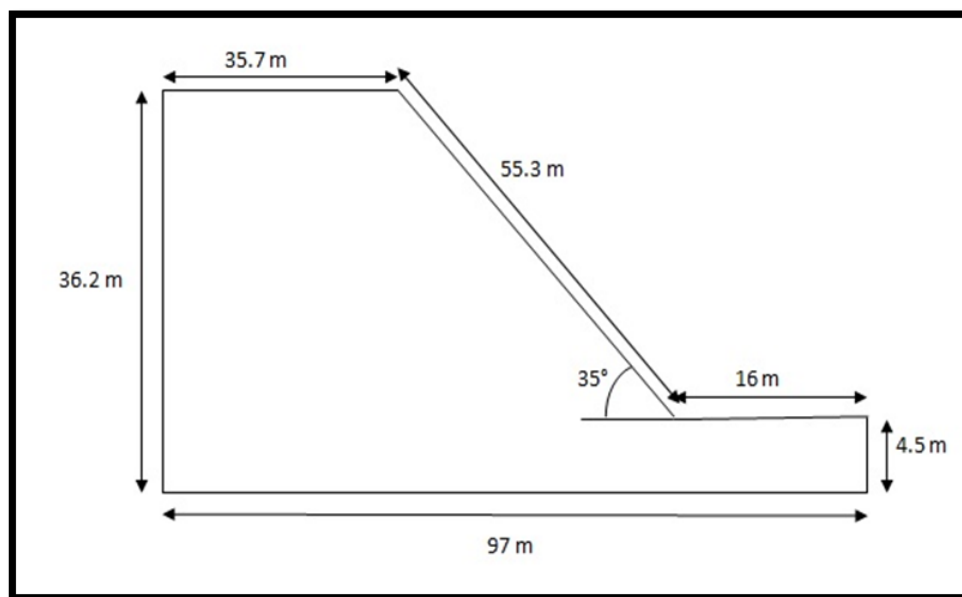


Fig. 3.3: Schematic diagram of slope

3.2.2 Geotechnical investigation of slope material

Soil samples were collected from different places at the study area to determine the properties of material of failure slope. By performing particle size distribution test in laboratory, the result shows that the material consist of sand, silt and clay and there are some fraction of stones are also available in non-homogeneous way and the gradation of

slope material comes as non-uniform as there was wide range of particle present. The soil is classified as silty sand in nature. Proportion of material found in parent soil is as follows (Singh et al. 2017):

Silt = from 9.07 to 37.93%,

Sand = 60.07%

Clay =1.6 to 4.86%

3.2.3 Rainfall characteristics

As above stated that the study area comes under the catchment area of Satluj valley. Rainfall in this area is because of S-W monsoon due to Orographic mechanism. The S-W monsoon appears June-September along with maximum precipitation depth. The Rainfall data for the region were provided by Shimla regional center of Indian Meteorological Department (IMD), listed below:

**Table 3.1: Rainfall data of Shimla district
(Source: Meteorological Center, Shimla)**

Month	Precipitation in mm
Oct, 2016	32.6
Nov, 2016	13.9
Dec, 2016	28.3
Jan, 2017	69.1
Feb, 2017	70.3
March, 2017	80
April, 2017	48.3
May, 2017	65
June, 2017	104.7
July, 2017	226.9
Aug, 2017	189
Sept, 2017	113
Oct, 2017	32.6

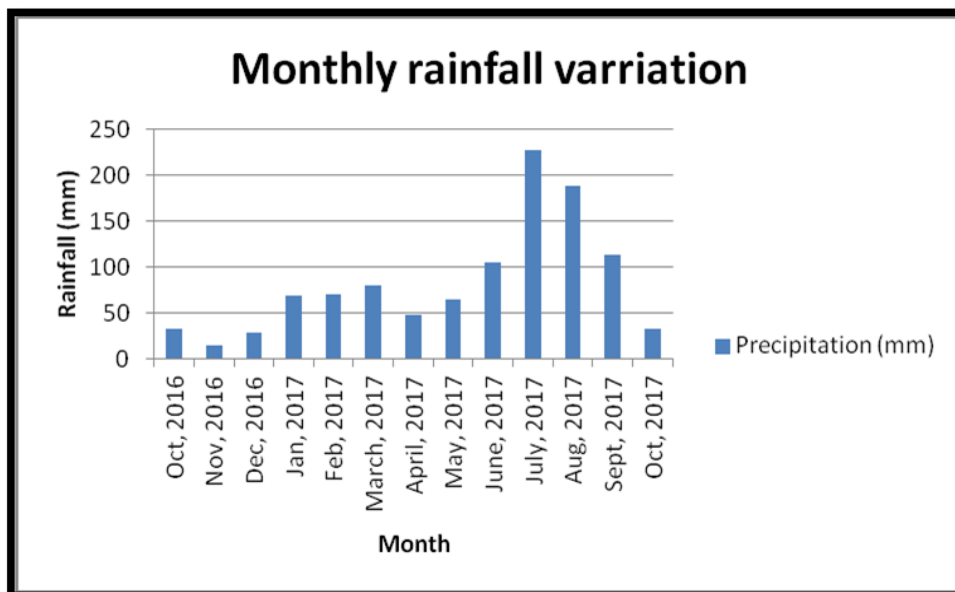


Fig. 3.4: Monthly precipitation variation
(Source: Meteorological Center, Shimla)

3.3 MATERIALS AND METHODS

In this study a model is adapted to study the mechanism of slope failure occurred in my study area. Further material is simulated by similar material theory.

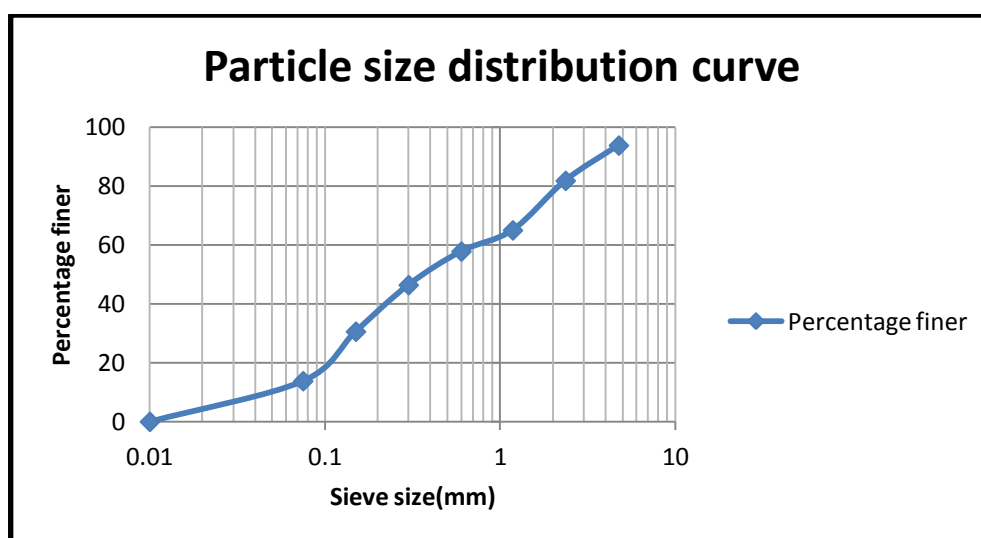
3.3.1 Material similarity and similar condition

Similar theory is used for the indoor model experiment. The experimental set-up and materials is prepared by similar criterion based on the Similar Theory. Similarity ratio is adopted according to the similar theory which is the ratio of prototype to model for the parameters. Which is geometric similarity ratio, quality similarity ratio, loading similarity ratio and boundary condition similarity ratio. (Terzaghi 1950; Skempton 1985; Yuan 1998).

The scale based physical model is mostly used models than any other mechanical models to study the landslide mechanism. So, model test used for the study of landslide should have own similarity characteristics. Which include dead load similarity, slope material similarity, rainfall duration similarity, and boundary condition similarity. These factors are effective parameters in physical model test used to study landslide mechanism.

Table 3.2: Sieve analysis of DTU soil

Sieve size in 'mm'	Retained weight in 'gm'	% weight retained	Cumulative % retain	% finer
4.75	31	6.2	6.2	93.8
2.36	60	12	18.2	81.8
1.18	84	16.8	35	65
0.6	36	7.2	42.2	57.8
0.3	57	11.4	53.6	46.4
0.15	79	15.8	69.4	30.6
0.075	84	16.8	86.2	13.8
Less than 0.075	69	13.8	100	0

**Fig. 3.5: Particle size distribution curve for DTU soil**

By above results, we can say that, Soil available in laboratory (DTU soil) constitutes 80% sand and 20% silt and clay which show that the DTU soil is classified as Sandy in nature. The study area constitutes major part of silt ranging from 19.07 to 37.93%, sand 60.07% and clay 1.6 to 4.86%. By approximation, we can take silt and clay together as 40% and sand as 60%. So, to meet the similarity condition 10% sand and 40% clay is added in the DTU soil and so the soil we get is Sandy in nature. As in study area there are stones and boulders are also present in debris material, so we mix 5% stones and boulders of different sizes to meet up with similarities. By material similarity, the similar ratio of cohesion, inner friction angle, modulus of Elasticity, and Poisson's ratio are taken similar to prototype, as $C_c = C_\phi = C_E = C_\mu = 1$. Figures of material used to meet up the similarity condition are shown below:



Fig. 3.6: Clay



Fig. 3.7: Stone and boulders



Fig. 3.8: DTU soil

3.3.2 Laboratory investigation

Laboratory investigation has been done to find the properties of soil for the analysis of slope stability.

3.3.2.1 Water content

It is found in laboratory by oven dry method. It is the most accurate method which is used for the determination of water content of the soil in the laboratory. It involves the weighing of the empty container (M_1) in which the most sample of the soil is placed and the container is again being weighted (M_2). The container is then placed in temperature controlled oven for drying of sufficient duration. For inorganic soil is carried out in the range of 105°C to 110°C and drying is done for 24 hours in order to ensure that the complete removal of the moisture from the sample and weight of the container with dry sample of soil is again noted (M_3).

$$\text{Water content} = \frac{\text{Mass of water}}{\text{Mass of solid}} \times 100 \quad (3.1)$$

$$\begin{aligned} \text{Where, Mass of water} &= M_2 - M_3 \\ \text{Mass of solid} &= M_3 - M_1 \end{aligned}$$

3.3.2.2 Particle size distribution

A sieve analysis (or gradation test) is a procedure used to assess the particle size distribution of a granular material by allowing the material to pass through a series of sieves of progressively smaller mesh size and weighing the amount of material that is stopped by each sieve as a fraction of the whole mass.

The gradation analysis in the coarse sand is determined using Sieve Analysis as per IS 2720 part 4. A gradation test is performed on a sample of aggregate in a laboratory. A typical sieve analysis involves a nested column of sieves with wire mesh screen. Percentage of different size of particles present in given dry sample is formed by particle size analysis. Sieve analysis is generally being carried out for coarse grained

soil. Sieve analysis is the true representative of particle size distribution as it is independent of the temperature. Sieve analysis is done for the particles having size greater than 0.075 mm that is for all soil fractions which are retained over 75 micron sieve.

According to IS 460:1962 sieves are designated terms of size of the openings are in mm. In the sieve analysis, different sieve arranged one over each other in the vertical plane with the sieves having maximum size of openings at the top and minimum size of opening at the bottom. A suitable amount (500 gm) of oven dried sample of the soil is placed over the top most sieve and sieving is done 10 minutes either manually or in sieve shaker. Sieve size used in my test includes 75 Micron, 150 Micron, 212 Micron, 300 Micron, 425 Micron, 600 Micron, 1 mm and 2 mm and arranged as shown in fig. 3.9

$$\text{Percentage finer} = 100 - \text{Percentage retained} \quad (3.2)$$

The result of the sieve analysis is expressed in the terms of percentage finer and the corresponding size of the particle on log scale and results of test will be disused in next chapter.



Fig. 3.9: Sieve shaker

3.3.2.3 Specific Gravity

It can be determined by using pycnometer method as per IS 2720 part 3.

Procedure-

- Mass of empty pycnometer is noted (M1).
- An oven dried sample of soil is placed in the pycnometer and the mass of pycnometer is again noted (M2).
- Empty volume of the pycnometer is filled with the water in multiple stages along with the subsequent removal of air either by use of vacuum or by continuous stirring of sample. Mass of pycnometer filled with water is again noted (M3).
- Pycnometer is completely emptied and again we filled with water after its proper cleaning and is again weighted (M4).
- The results of test will be disused in next chapter.



Fig. 3.10: Pycnometer

Specific gravity $G = \frac{\text{Mass of solid of given volume}}{\text{Mass of water of same volume}}$

$$G = \frac{(M_2 - M_1)}{(M_4 - M_1)(M_3 - M_2)} \quad (3.3)$$

3.3.2.4 Triaxial test

The triaxial test is carried out in a cell on a cylindrical soil sample having a length to diameter ratio of 2. Three principal stresses are applied to the soil sample, out of which two are applied water pressure inside the confining cell and are equal. The third principal stress is applied by a loading ram through the top of the cell and is different to the other two principal stresses. A typical triaxial cell is shown.

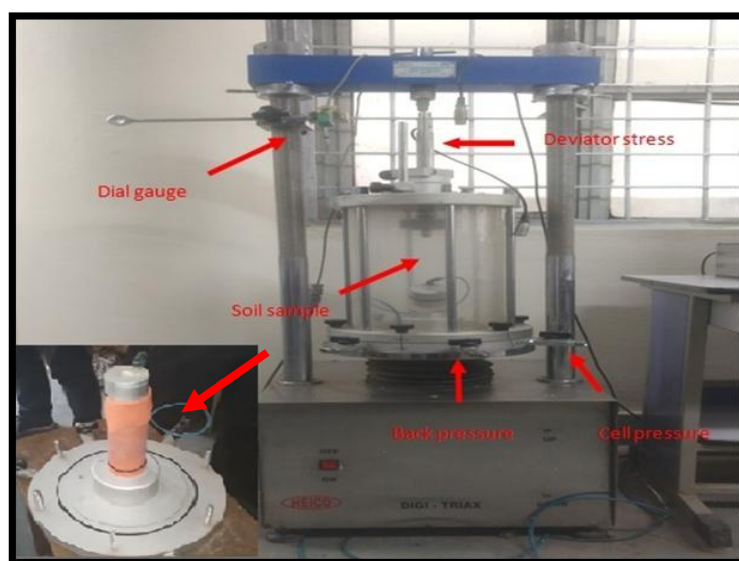


Fig. 3.11: Triaxial test set-up

The soil sample is placed inside a rubber sheath which is sealed to a top cap and bottom pedestal by rubber O-rings. For tests with pore pressure measurement, porous discs are placed at the bottom, and sometimes at the top of the specimen. Filter paper drains may be provided around the outside of the specimen in order to speed up the consolidation process. Pore pressure generated inside the specimen during testing can be measured by means of pressure transducers.

The triaxial compression test consists of two stages:

First stage: In this, a soil sample is set in the triaxial cell and confining pressure is then applied.

Second stage: In this, additional axial stress (also called deviator stress) is applied which induces shear stresses in the sample. The axial stress is continuously increased until the sample fails.

During both the stages, the applied stresses, axial strain, and pore water pressure or change in sample volume can be measured.

Test Types: There are several test variations, and those used mostly in practice are:

UU (unconsolidated undrained) test: In this, cell pressure is applied without allowing drainage. Then keeping cell pressure constant, deviator stress is increased to failure without drainage.

CU (consolidated undrained) test: In this, drainage is allowed during cell pressure application. Then without allowing further drainage, deviator stress is increased keeping cell pressure constant.

CD (consolidated drained) test: This is similar to **CU test** except that as deviator stress is increased, drainage is permitted. The rate of loading must be slow enough to ensure no excess pore water pressure develops.

3.3.2.5 Unit weight

There are several types of test which can be used to study the compactive properties of soils. Because of the importance of compaction in most earth works standard procedures have been developed. These generally involve compacting soil into a mould at various moisture contents. It is generally of two types:

1. Standard Compaction Test
2. Modified Compaction Test

In my experimental test I used standard proctor test to find the bulk density of my test soil sample in this test soil is compacted into a mould in 3-5 equal layers, each layer receiving 25 blows of a hammer of standard weight. The apparatus is shown in Figure

below. The energy (compactive effort) supplied in this test is 595 kJ/m³. The important dimensions are:

Volume of mould = 1000 cm³

Hammer mass = 2.5 kg

Drop of hammer = 300 mm

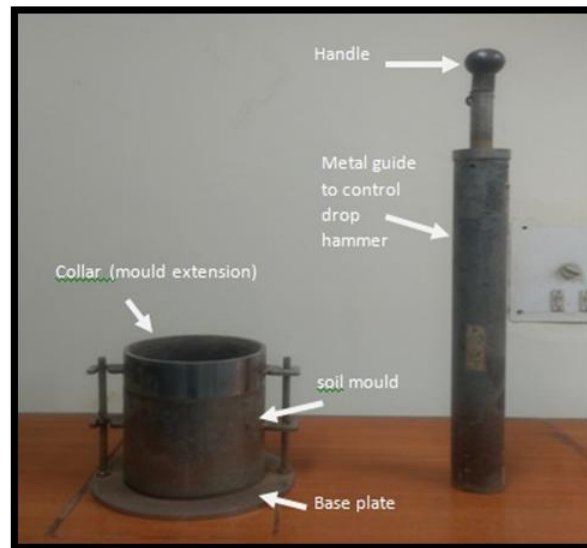


Fig. 3.12: Standard proctor test

According to similarity conditions the water added to find the bulk unit weight of testing soil is kept same as of the parent material. Using standard proctor test bulk unit weight of the soil has been found by the following:

$$\text{Bulk unit weight}(\gamma_b) = \frac{W}{V} = \frac{W_s + W_w}{V} \quad (3.4)$$

$$\text{Dry unit weight}(\gamma_d) = \frac{\gamma_b}{1+w} = \frac{G \gamma_w}{1+e} \quad (3.5)$$

$$\text{Saturated unit weight}(\gamma_s) = \frac{(G+e)\gamma_w}{1+e} \quad (3.6)$$

Where:

W=weight of soil; W_s = weight of solids; W_w = weight of water; V = Total volume of soil; γ_w = unit weight of water; w = water content e = void ratio

3.3.2.6 Permeability of soil

It is the ability of the medium which permit the flow of the fluid through its interconnecting void. Permeability of coarse grained soil is more than the permeability of fine grained soil as follows:

Table 3.3: Permeability range for different soil
(Source: Lewis et al. 2006)

Types of soil	Permeability (K)
Gravel	> 1
Sand	$1 - 10^{-3}$
Silt	$10^{-3} - 10^{-7}$
Clay	$< 10^{-7}$

As per Darcy law for laminar flow condition in saturated soil mass proportional to hydraulic gradient and so the permeability may also be defined as rate of flow through the medium per unit area under unit hydraulic gradient.

$$Q = KiA \quad (3.7)$$

Where; Q = Discharge through soil voids

i = Hydraulic gradient

A = Cross-sectional area of soil medium

Falling head method: For fine grained soil permeability is found by falling head method. In this method a stand pipe of known area is inserted in soil sample to be tested and flow is allowed to take place through it into the sample. over a period of time the height of the water in the stand pipe reduces due to the flow of the water place through it into the sample. The height of the water in the stand pipe at different time is noted to find the permeability of the given sample of the soil. The test setup and formula used is shown in fig. Below:

$$K = \frac{2.303 a L \log_{10} \left(\frac{h_1}{h_2} \right)}{A t} \quad (3.8)$$

Where; t = Time taken by the flow to reduce the height from h_1 to h_2 .

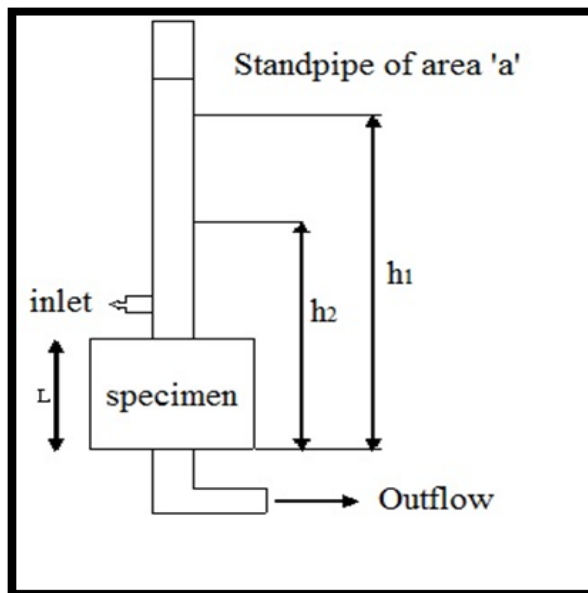


Fig. 3.13: Schematic diagram of Falling head test set-up

3.3.3 Experimental set-up

Schematic diagrams of setup used in the physical study of rainfall induced landslide are introduced in this section to provide an idea of model and test equipment. This section is the key to direction towards the implementation of whole physical modelling and experiments performed in the study.

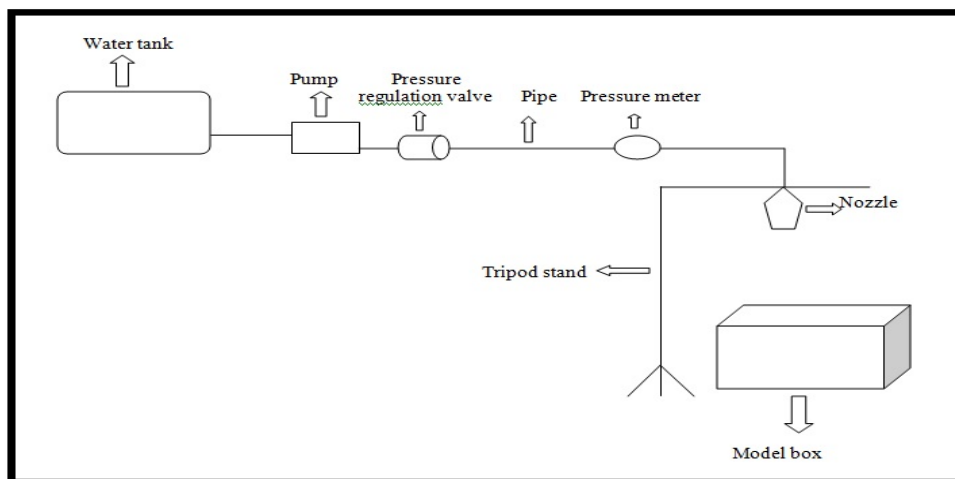


Fig 3.14: Schematic diagram of experimental setup

3.3.3.1 Experimental platform

The experimental platform is to be designed as frame-type model using transparent acrylic sheet of 15mm thickness. The experimental setup includes experimental platform system and a self made artificial rainfall system. The similarity ratio of geometry $C_G = n$. In this test, the geometry scale is taken 10 as the prototype is large in size. The experimental platform is a cube tank, which measures 97 cm long, 57 cm wide, and 48.5 cm high. By taking scale of

$$1\text{cm} = 1\text{ meter}$$

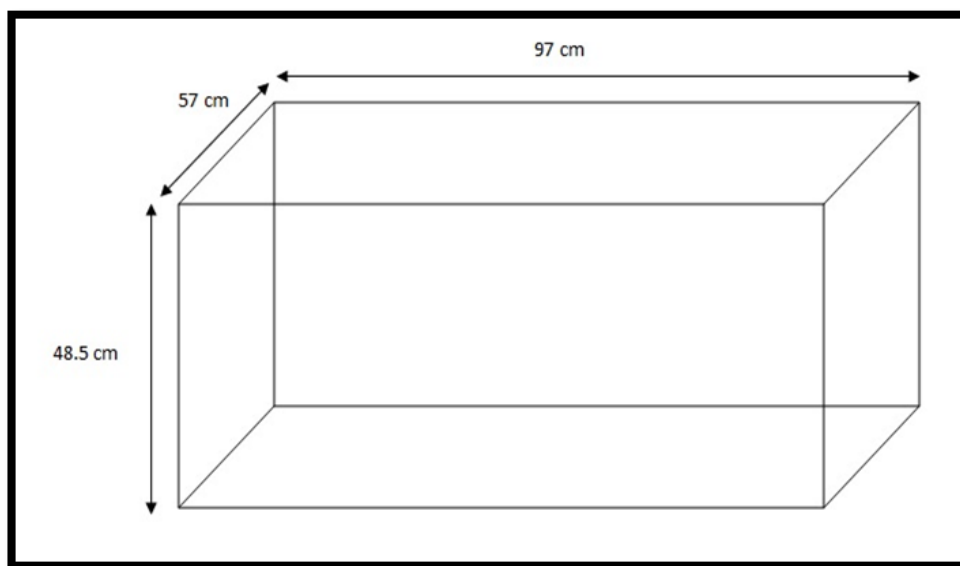


Fig. 3.15: Schematic diagram of test model

3.3.3.2 Rainfall generator

An artificial rainfall generator is to be designed to simulate the rainfall characteristics. Rainfall generator includes a water supply tank, a submersible pump, a pressure regulating valve to control pressure of pump, a pressure meter to measure the pressure of water flow and a nozzle to generate raindrop. The water is sprayed by the pump on the top of experimental platform. The spray device is designed to simulate different rainfall intensity using control valve. The schematic diagram of rainfall generator is shown below-

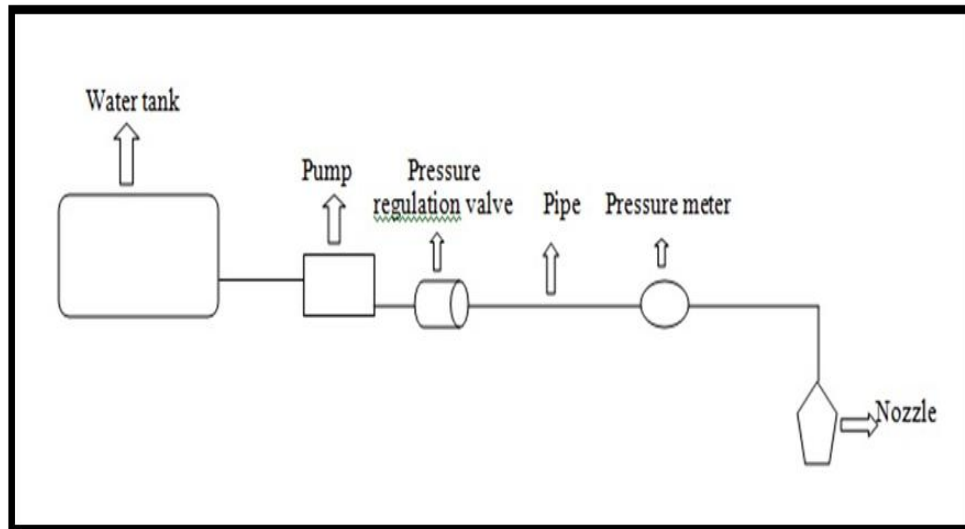


Fig. 3.16: Schematic diagram of rainfall generator

The rainfall process includes three parameters-

- a) Rainfall intensity
- b) Rainfall duration
- c) Rainfall interval.

The rainfall duration and rainfall interval both depends on time factor. The relationship between rainfall intensity and the total rainfall is -

$$q = \frac{Q}{t} \quad (3.9)$$

Where:

q = rainfall intensity; t = is rainfall duration; Q = is total rainfall in the rainfall duration.

CHAPTER 4

PHYSICAL MODELLING

4.1 GENERAL

It is very difficult to describe loess landslide only with a mathematical model due to sudden failure, complexity and unpredictability. So the physical model test is a more effective and widely used method to explore the sliding mechanism to investigate water movement, analyze rainfall-induced slope instability, and then forecast and control landslides (Sanchi's et al. 2013).

Landslide frame model is one of the most commonly used test methods. The model is constructed using similar material in the framework model slot in which parameters such as stress, deformation and other mechanical properties can be measured to meet the similarity to prototype. The sliding characteristics and mechanism can be observed, and some mechanical parameters such as stress and strain displacement can be obtained quantitatively through landslide frame model (Iverson 2000; okura et al. 2002; Take 2004; Cascini et al. 2010, 2013).

Based on the previous research, a physical model test is implemented in this study under the same engineering background. The basic mechanical properties of similar materials are tested and derived through the dimensional method. The similar conditions of physical model experiment were obtained according to the Similar Theories. The start-up conditions and sliding mechanism of rainfall-induced landslide is studied through physical model experimental method.

4.2 EXPERIMENTAL SET-UP

As explained in previous section of experimental set-up, the experimental platform includes Model box and an artificial rainfall system. So frame-type model box and a self made rainfall generating system are designed and explained below. Results of test performed are shown in next chapter.

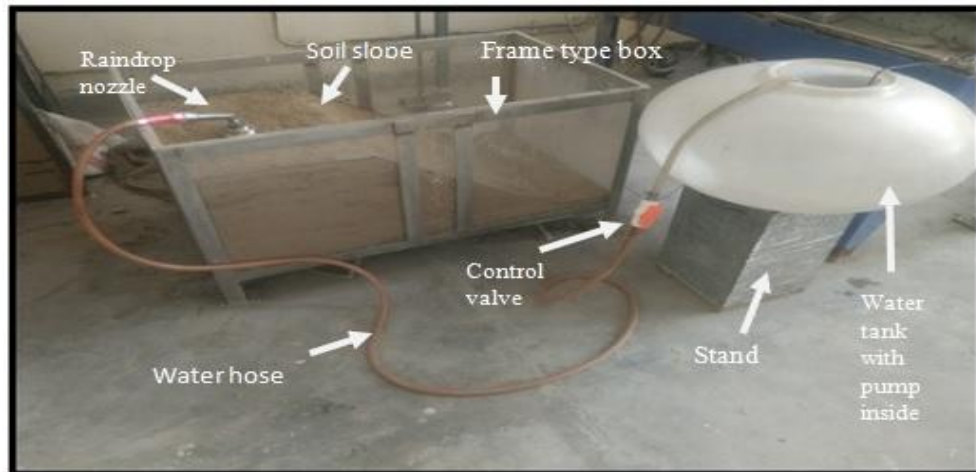


Fig. 4.1: Experimental set-up

4.2.1 Frame type box

The frame type model is designed using transparent acrylic sheet of 15mm thickness is for experimental work. The similarity ratio of geometry $C_G = n$. In this test, the geometry scale is taken 10 as the prototype is large in size. The experimental platform is a cube tank, which measures 97 cm long, 57 cm wide, and 48.5 cm high. By taking scale of:

$$1\text{cm} = 1 \text{ meter}$$



Fig. 4.2: Frame type box with marking on it according to Jhakri slope

Further, the soil is filled in designed box according to slope size described from Jhakri slope in my study area as shown below:



Fig. 4.3: Frame type model with soil slope

4.2.2 Rainfall generator

According to schematic diagram shown in previous chapter a artificial rainfall generator is designed including water tank, submersible pump, control valve, and raindrop nozzle as shown below:



Fig. 4.4: Rainfall generator

4.2.2.1 Pump

To generate a desired rainfall depth with varying pressure is installed in rainfall generator. The discharge capacity of pump is 0.05 liter/sec which is 0.18m³/hr and for the slope area which is 0.6099 m², the intensity of rainfall is 295 mm/hr.



Fig. 4.5: Submersible pump

4.2.2.2 Flow regulating valve

To control the flow of water a sluice valve is attached to the rainfall generator having scales drawn on it. The hand wheel is rotated to increase or decrease the flow as needed, further marking is done according to need in our experimental platform

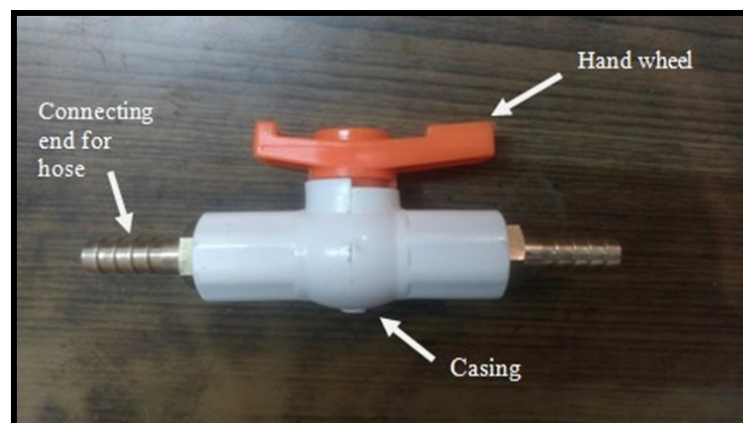


Fig. 4.6: Flow regulating valve

4.2.2.3 Raindrop nozzle

For the generation of rainfall a nozzle is installed in rainfall generator to simulate the rainfall. It has fixed type perforated openings so the size of water droplets cannot be changed which is also a type of restriction in this modelling as in real rainfall the size of droplets varies. The diameter of perforated plate is 8cm.

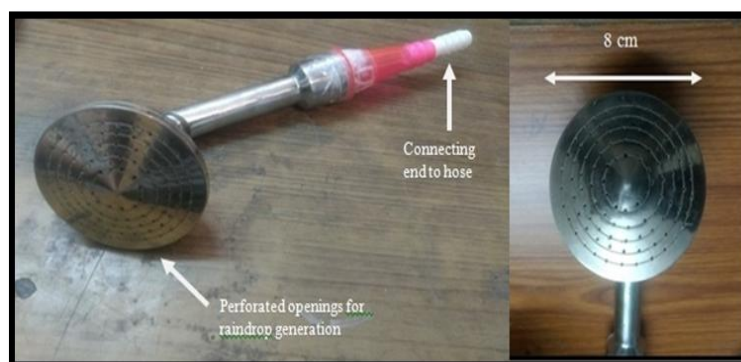


Fig. 4.7: Raindrop nozzle

The rainfall depth is kept to 10 mm in each rainfall till the failure takes place and variable interval of 15 min, 30 min, 45 min and 60 min is kept for next successive rainfalls to make moisture infiltrate properly. To generate the rainfall of 10mm depth the volume of water is calculated which is equal to total slope area multiplied by rainfall depth.

$$\begin{aligned}
 \text{So, volume of water for 10mm rainfall} &= (0.6099\text{m}^2) * (10*10^{-3} \text{ m}) \\
 &= 0.006099\text{m}^3 \\
 &= 6.099 \text{ liter} \\
 &= 6.1 \text{ liter (approx.)}
 \end{aligned}$$

By above calculation it is clear that for this particular slope model 6.1 liter water is needed to generate the 10mm depth of rainfall as in my test the tank is filled with same amount of water each time to generate the 10 mm depth of rainfall.

CHAPTER 5

NUMERICAL MODELLING

5.1 GENERAL

Slope stability analysis deal with calculation, investigation, modelling and design of natural and artificial rock and soil slopes. Slope stability analysis is performed to assess the safe design of a human-made or natural slopes e.g. embankments, road cuts, open-pit mining, excavations, landfills etc. and the equilibrium conditions. Slope stability is the resistance of inclined surface to failure by sliding or collapsing. The main objectives of slope stability analysis are finding endangered areas, investigation of potential failure mechanisms, determination of the slope sensitivity to different triggering mechanisms, designing of optimal slopes with regard to safety, reliability and economics, designing possible remedial measures, e.g. barriers and stabilization.

Successful design of the slope requires geological information and site characteristics for example basic properties of soil and rock mass, slope geometry, groundwater conditions, alternation of materials by faulting, joint or discontinuity systems, movements and tension in joints, earthquake activity etc. The presence of water has detrimental effect on slope stability. Water pressure acting in the pore spaces, fractures or other discontinuities in the materials that make up the pit slope will reduce the strength of those materials. Choice of correct analysis technique depends on both site conditions and the potential mode of failure, with careful consideration being given to the varying strengths, weaknesses and limitations inherent in each methodology.

In my study, analysis has been done by Modified Bishop's Method of Analysis. The method is discussed below:

Modified Bishop's method of analysis- The Modified Bishop's method is slightly different from the ordinary method of slices in that normal interaction forces between adjacent slices are assumed to be collinear and the resultant inter-slice shear force is zero. The approach was proposed by Alan W. Bishop of Imperial College. The constraint introduced by the normal forces between slices makes the problem statically indeterminate. As a result, iterative methods have to be used to solve for the factor of safety. The method has been shown to produce factor of safety values within a few percent of the "correct" values. The factor of safety for moment equilibrium in Bishop's method can be expressed as

$$\mathbf{FS} = \frac{\sum_j \frac{[c' l_j + (W_j - u_j l_j) \tan \varphi']}{\psi_j}}{\sum_j W_j \sin \alpha_j} \quad (5.1)$$

$$\text{Where: } \psi_j = \cos \alpha_j + \frac{\sin \alpha_j \tan \varphi'}{\mathbf{FS}}$$

Here \mathbf{j} is the slice index, \mathbf{c}' is the effective cohesion, φ' is the effective internal angle of internal friction, \mathbf{l} is the width of each slice, \mathbf{W} is the weight of each slice and \mathbf{u} is the water pressure at the base of each slice. An iterative method has to be used to solve for \mathbf{FS} because the factor of safety appears both on the left and right hand sides of the equation. so in my study analysis has been done using **GEO5(Demo version) software**. The geometry and material properties of the slope is taken according to the model test as mentioned.

5.2 SLOPE STABILITY ANALYSIS BY GEO5 SOFTWARE

5.2.1 Introduction

GEO5 contains several programs for analyses of soil and rock slopes, dams, newly built embankments, and check of retaining walls global stability. The basic

program for stability analysis is Slope Stability. It enables design and analysis of slope stability with circular or polygonal surface and automatic optimization of slip surface. It co-operates with all programs for analysis of Excavation Designs and Retaining Wall Designs. It enables creation of anchors, geo-reinforcements, surcharge and earthquake effects modelling.

5.2.2 Procedure

1. In the frame “Settings” click on “Select settings” and choose option No. 1 – “Standard – safety factors”. Then, in the frame “Interface” click on “Setup ranges” and input the coordinate range.

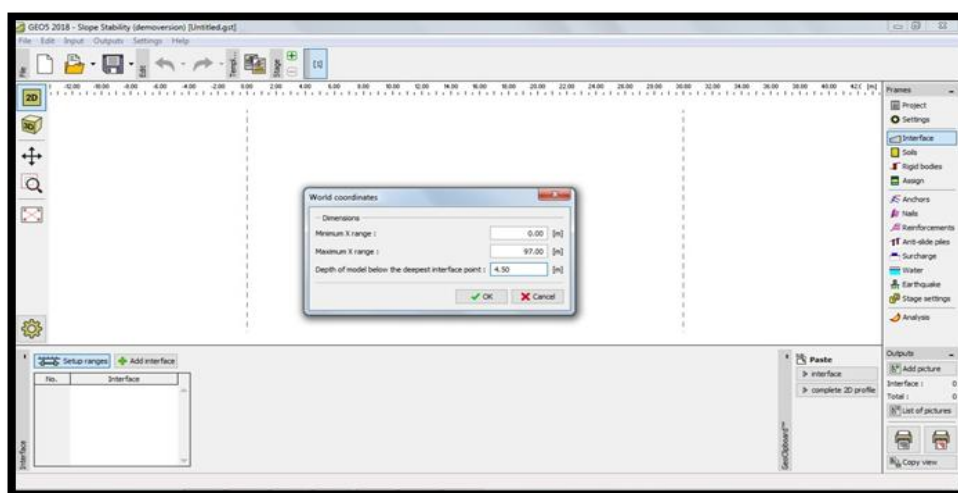


Fig. 5.1 Co-ordinate range set-up

2. Then click on “Add interface” to model the interface of layers, using the coordinates. For each interface, add all points of the interface textually and then click on “OK Add interface”

Table 5.1: Co-ordinates of interface of soil layers

S.No	Interface 1		Interface 2	
	X in m	Z in m	X in m	Z in m
1	0	0	0	31.7
2	81	0	35.7	31.7
3	97	0	81	0

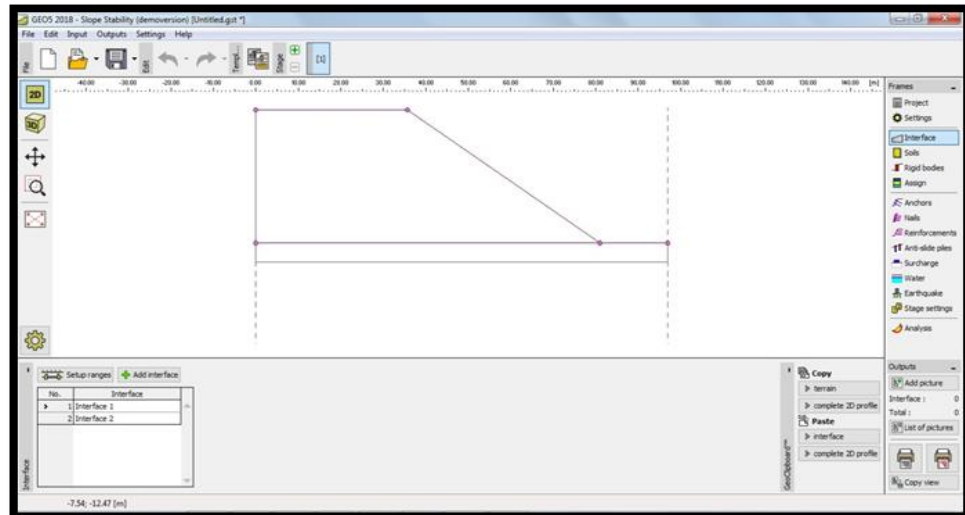


Fig. 5.2: Interface of soil layer

3. Then add soils with the parameters of Test soil found from laboratory using the button “Add” and assign the soils.

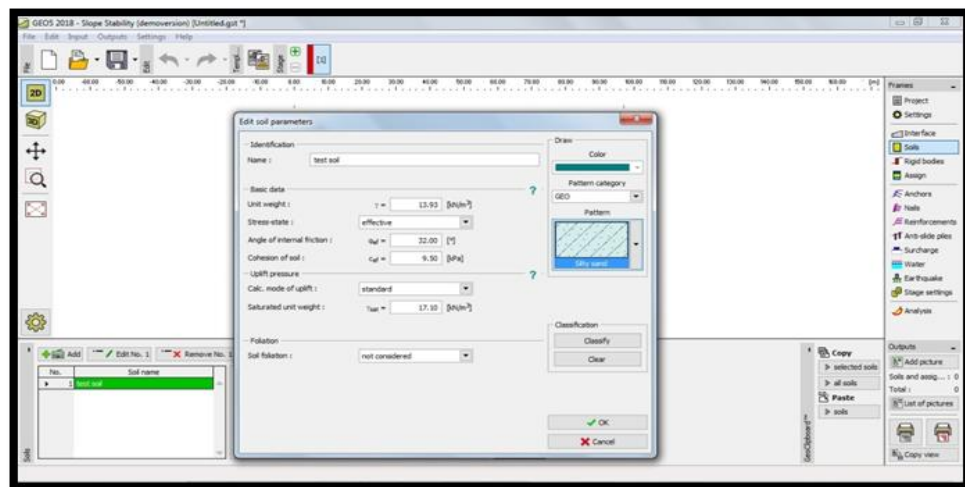


Fig. 5.3: Assigning of soil

4. Now open the frame “Analysis”, where you can enter the initial slip surface using the coordinates of the center (x, y) and its radius or using the mouse – by clicking on the interface to enter three points through which the slip surface passes.

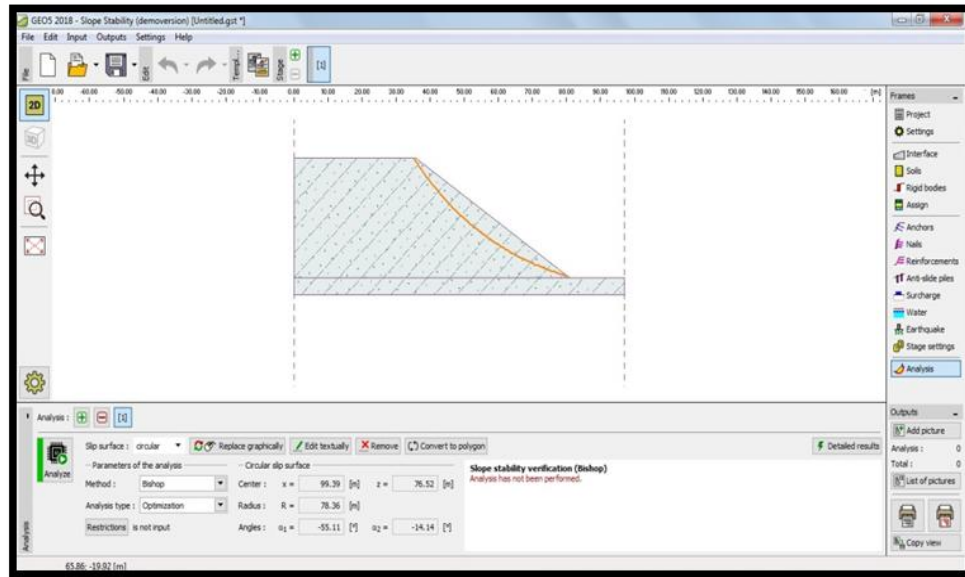


Fig. 5.4: Inputting Slip surface

5. After inputting the initial slip surface, select “Bishop” as the analysis method and then set the type of the analysis to “Optimization”. Then perform the actual verification by clicking on “Analyze”. Optimization consists of finding the circular slip surface with the lowest stability – the critical slip surface. The optimization of circular slip surfaces in the Slope stability program evaluates the entire slope and is very reliable.
6. The level of stability defined for the critical slip surface using the “Bishop” evaluation method is not satisfactory ($SF = 1.28 < SF = 1.5$)

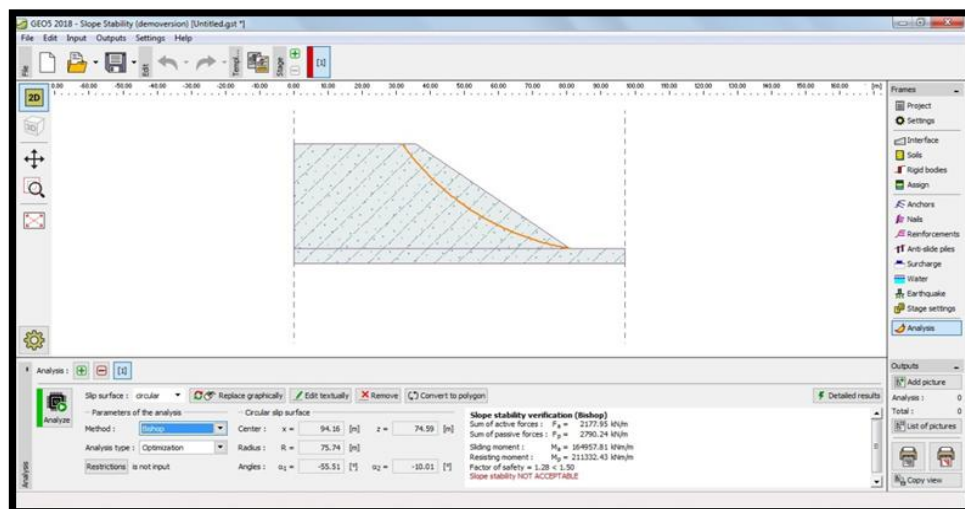


Fig. 5.5 Stability analysis of slope by Bishop Method

As we can clearly see that the slope is not initially stable as factor of safety for the critical failure plane is $F=1.28$ (which is less than 1.5). So in this experiment we will see that how rainfall triggers the landslide and damages the slope. Comparison of physical failure pattern has been done with this numerical slip failure surface. The study provides a threshold rainfall depth at which failure takes place by the action of rainwater which further helps in monitoring and early warning of slope failure.

CHAPTER 6

RESULTS AND DISCUSSION

6.1 LABORATORY RESULTS

Laboratory investigation has been done to find the properties of soil for the analysis of slope stability and to meet the material similarity of soil. Different physical and engineering properties of the soil are obtained by conducting different tests. Results of the tests discussed in this section.

Table 6.1: Soil properties

	Moisture content 'w'	bulk Density 'ρ' in gm/cc
DTU soil	5.92 %	1.75
Clay	6.32 %	1.43
Sand	9.04 %	1.5

Table 6.2: Properties of experimental soil obtained by similar material condition

Bulk unit weight at 5% water content (KN/m ³)	13.93
Dry unit weight (KN/m ³)	13.3
Saturated unit Weight (KN/m ³)	17.1
Specific gravity	2.64
Coefficient of permeability(m/hr)	0.0023
Cohesion (kg/cm ²)	9.5
Angle of internal friction (φ °)	32

6.2 PHYSICAL MODELLING TEST RESULT

The effect of rainfall on slope with 10 mm rainfall depth variation is shown below to visualize the failure pattern of the slope.

6.2.1 At 10mm rainfall depth- At 10mm rainfall depth rainwater percolation takes place at faster rate.



Fig. 6.1: Effect of rainfall at 10 mm depth

6.2.2 At 20mm rainfall depth-At 20mm rainfall depth the water percolation still takes place along with surface runoff.



Fig. 6.2: Effect of rainfall at 20 mm depth

6.2.3 At 30mm rainfall depth- At 30mm rainfall depth percolation takes place at slower rate and due to increase in runoff water, erosion of slope starts.



Fig. 6.3: Effect of rainfall at 30 mm depth (side view)



Fig. 6.4: Effect of rainfall at 30 mm depth (top view)

6.2.4 At 40mm rainfall depth- At 40mm rainfall depth water percolation continues at slower rate as shown in fig. but due to heavy runoff water erosion of slope become major.



Fig. 6.5: Effect of rainfall at 40mm depth (side view)



Fig. 6.6: Effect of rainfall at 40 mm (top view)

6.2.5 At 50mm rainfall depth- At 50mm depth as we can see in following figure the percolation continues but due to erosion, slope is getting critical.



Fig. 6.7: Effect of rainfall at 50mm depth (side view)



Fig. 6.8: Effect of rainfall at 50 mm depth (top view)

6.2.6 At 60mm rainfall depth- At 60 mm rainfall depth as we can see the percolation process becomes very slow thus accumulation of water takes place which leads to the increment in the pore water pressure which helps in erosion of slope as shear strength of soil getting weaker.



Fig. 6.9: Effect of rainfall at 60mm depth (side view)



Fig. 6.10: Effect of rainfall at 60 mm depth (top view)

6.2.7 At 70mm rainfall depth- At 70mm rainfall depth after giving time for percolation the soil is now fully saturated and slice failure near the toe of slope takes place due to the positive pore pressure generated.



Fig. 6.11: Effect of rainfall at 70mm depth (side view)



Fig. 6.12: Effect of rainfall at 70 mm depth (top view)

6.2.8 At 80mm rainfall depth- At 80 mm rainfall depth as the soil is already saturated the pore pressure increases and due to reduction of shear strength slope failure occurs as the weakest slip surface shown in numerical modelling.



Fig. 6.13: Effect of rainfall at 80mm depth (side view)



Fig. 6.14: Effect of rainfall at 80mm depth (top view)

6.3 NUMERICAL MODELLING TEST RESULT- Factor of safety before the rainfall using GEO5 software for the critical failure plane comes $F=1.28$ (which is less than 1.5). So failure should occur according to failure plane shown in stability analysis.

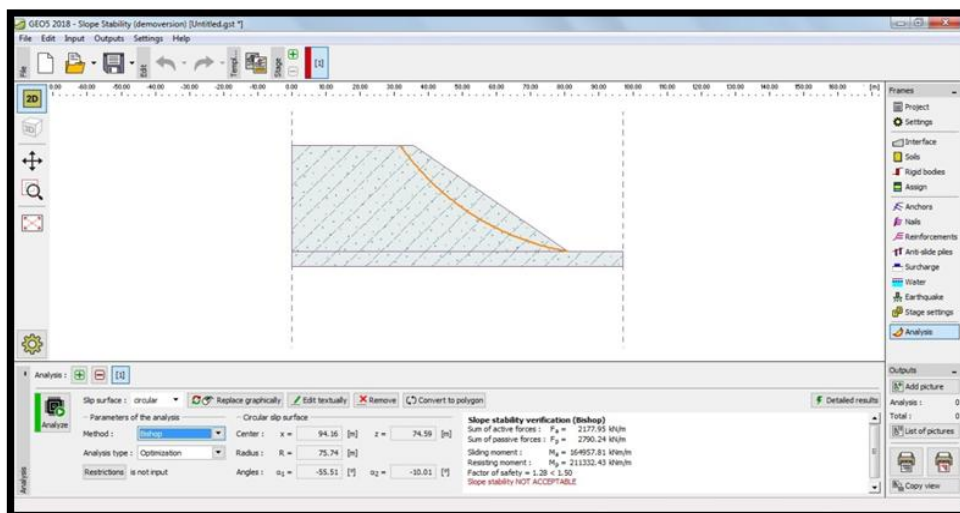


Fig. 6.15: Stability analysis of slope by Bishop Method (By using GEO5 2018 software)

At 80mm rainfall depth the soil sample is taken from the model and triaxial test is performed to find out the variation of stress and strain at 80mm rainfall depth as shown below:

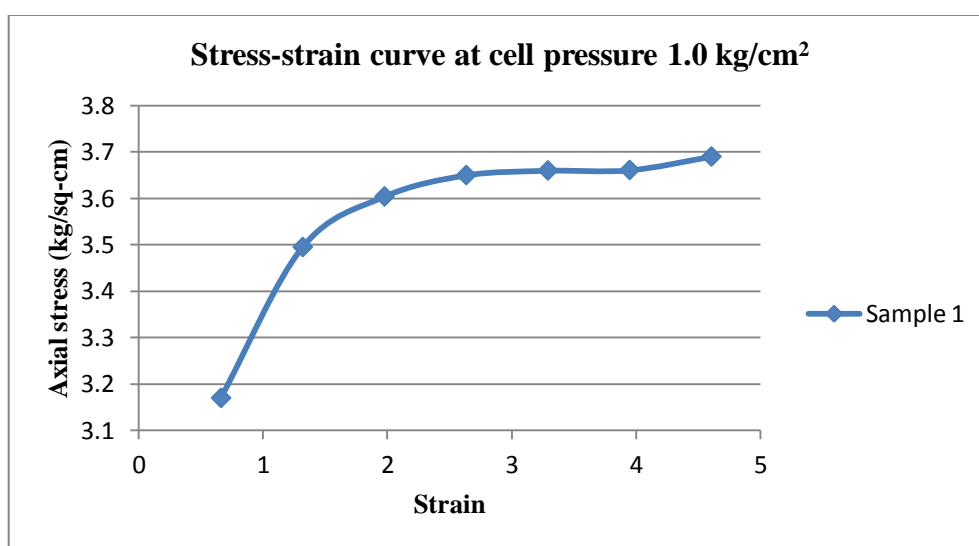


Fig. 6.16: Stress-strain behavior of soil at 80mm rainfall depth using triaxial test at cell pressure 1.0 kg/cm^2

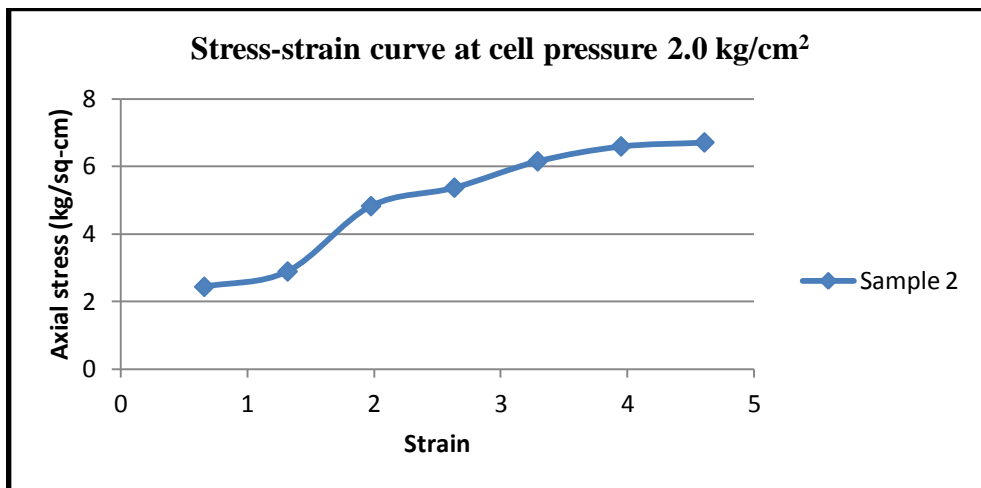


Fig. 6.17: Stress-strain behavior of soil at 80mm rainfall depth using triaxial test at cell pressure 2.0 kg/cm²

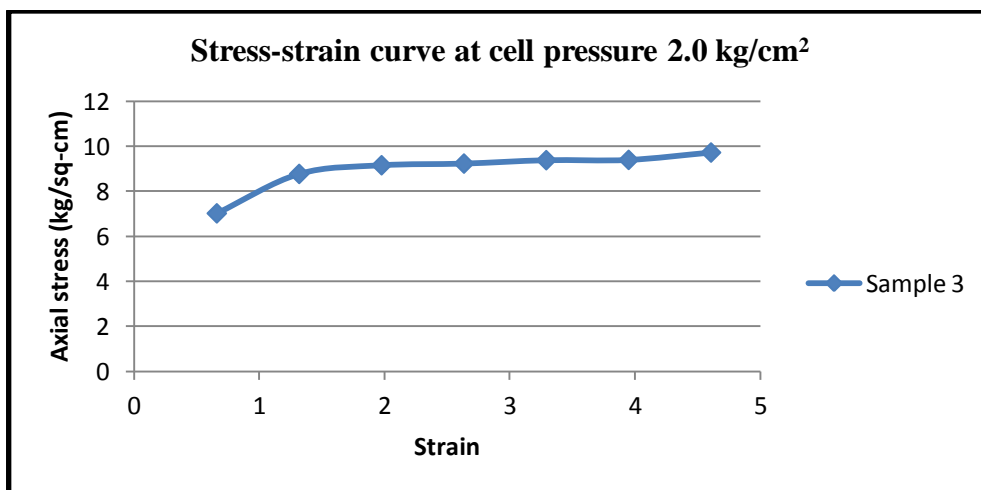


Fig. 6.18: Stress-strain behavior of soil at 80mm rainfall depth using triaxial test at cell pressure 3.0 kg/cm²

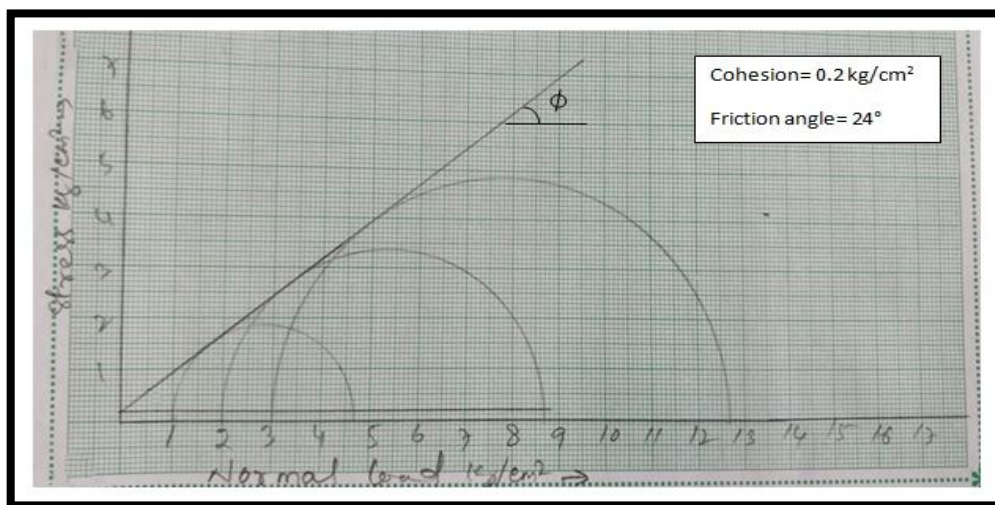


Fig. 6.19: Mohr circle for soil at 80mm rainfall depth using triaxial test

Using triaxial test data, cohesion and friction value has been found and using these parameters factor of safety of the existing failure slope has also been found using GEO5 software as following:

Table 6.3: Slope parameters at 80mm rainfall depth

Rainfall depth (mm)	Cohesion (kg/cm²)	Friction angle(ϕ)	Factor of safety
80	0.2	24°	0.66

Above results shows that the slice failure takes place at 80 mm rainfall depth as the factor of safety become very less (FS=0.66), which is less than 1 which justify the results.

6.4 DISCUSSION

According to this study the slice failure occurred at 80 mm rainfall depth although erosion failure starts at 30mm rainfall depth following the failure plane according to slip surface shown in numerical modeling which justify the results.

Probable initiation mechanism

A probable initiation mechanism for shallow landslides on steep slopes is developed which is Based on the above results of the slope characteristics, geotechnical properties of the soil, rainfall infiltration, shear strength of the soil, and soil behavior with the increase in rainfall depth,

- As heavy rainfall takes place, rain water infiltrates into the layer of soil and creates water level between the slopes which in turn increases the pore water pressure. The soil layer in the lower part will become fully saturated first because the thickness of the soil layer at the toe of slope is very less.

- As the hydraulic conductivity (k) of the soil is very less as compared to rainfall intensity. Most of the rain water converts into surface runoff which in turn leads to the erosion of the surface of the slope. This stage starts at 30mm rainfall depth.
- Further increase in rainfall depth i.e. at 40mm rainfall depth, erosion of soil surface increases rapidly which is considered as initiation of slope failure.
- Again continuous increase in rainfall depth vigorous erosion may occur, which results in removal of the soil layer in the lower part of the slope that provides the resistance for slope stability. Further, the water level in the slope keeps increasing due to the continuous rainfall infiltration, i.e. the pore water pressure in the soil keeps increasing and after reaching at critical stage sliding failure takes place. When the pore-water pressure exceeds the critical value, a shallow landslide triggered as a result of heavy rainfall. This stage occurred at 80mm rainfall depth and factor of safety is found very less (i.e. $FS=0.66$).

CHAPTER 7

CONCLUSION

7.1 CONCLUSION OF RESULTS

This study basically provides a scientific and theoretical guidance for early warning, monitoring, prevention, and control of the rainfall-induced landslide.

A physical model test on rainfall-induced landslides has been conducted in my study. A self-designed frame-type landslide model has been adopted, which includes experimental platform system and a self made artificial rainfall system. In my study, the soil materials are simulated by martial similarity theory from study site which is situated in JHAKRI town of Himachal Pradesh as this site has continuous slope failure in history.

The results of my study show that the methods used are an effective method to monitor the infiltration process of pore water. The sliding mechanism of slope and factors influencing slope failure has been studied in this thesis. Start-up conditions of slope failure are as follows:

- The intensity of rainfall is about 295 mm/hr and rainfall of 10mm depth is introduced each time;
- surface erosion is more likely to occur initially than the internal landslide,

The main triggering factor for shallow landslides on the Jhakri slope is the high-intensity rainfall which generates heavy runoff water because of the heavy runoff water soil erosion takes place which helps in initiation of slope failures and further rainfall

continuity turned into landslide. On the steep slopes due to occurrence of shallow landslides the sliding mass transformed into debris flows during heavy rainfall which in turn causes loss to life and property.

By analyzing the soil behavior with respect to increase in rainfall depth show that failure of the slope did not occur until the pore water pressure exceeds a relatively high value. So this study explains that why steep slopes can be stable under low intensity rainfall during the rainy season. However, if the pore-water pressure exceeds the critical value as a result of heavy rainfall, shallow landslides will be triggered due to reduction in shear strength of soil.

The above proposed probable initiation mechanism indicates that the initial failure process of the shallow landslides on Jhakri slope begins with surface erosion caused by surface runoff. The combination of loss of resistance force of the slope and increase in pore-water pressure in the slope during heavy rainfall are main factors making the slope to a critical condition.

7.2 FUTURE SCOPE OF THIS PROJECT

However, there are some limitations existing in my study as the geometric size of landslide prototype is relatively very large while the size of the laboratory model is limited in terms of the testing feasibility and in data collection there may be some imperfection present. All these limitations are supposed to be improved in the subsequent research. The results show rainfall-induced landslides mechanism, and still need to be verified in the engineering practice. However, this study basically provides a scientific and theoretical guidance for early warning, monitoring, prevention, and control of the rainfall-induced landslide.

REFERENCES

- [1]. Abramson, L.W., Lee, T.S., Sharma, S., Boyce, G.M. (2002). "Slope stability and stabilization methods." 2nd edn. Wiley, New York
- [2]. Acharya, K.P., Bhandary, N.P., Dahal, R.K., Yatabe, R. (2015). "Numerical analysis on influence of principal parameters of topography on hillslope instability in a small catchment." *Environ Earth Sci.*, 73:5643–5656
- [3]. Bartarya, S.K., Valdiya, K.S. (1989). "Landslides and erosion in the catchment of the Gaula River, Kumaun Lesser Himalaya, India." *Mt Res Dev* 9(4):405–419
- [4]. Bartarya, S.K., Viridi, N.S., Sah, M.P. (1996). "Landslide hazards: some case studies from the Satluj Valley, Himachal Pradesh." *Himalayan Geol* 17:193–207
- [5]. Behera PK, Sarkar K, Singh AK, Verma AK, Singh TN (2016) "Dump slope stability analysis - a case study." *J Geol Soc India* 88(6):725–735
- [6]. Budhu, M.; Gobin, R. (1996) "Slope Instability from Ground-Water Seepage." *Journal of Hydraulic Engineering*:415_417.
- [7]. Cascini L, Cuomo S, Pastor M, Saccoa G (2013) "Modelling the postfailure stage of rainfall-induced landslides of the flow type." *Can Geotech J* 50(9):924–934.
- [8]. Cascini L, Cuomo S, Pastor M, Sorbino G (2010) "Modelling of rainfall-induced shallow landslides of the flow-type." *J Geotech Geoenviron Eng* 1(136):85–98.
- [9]. Chandrasekaran, S.S., Oweise, R.S., Ashwin, S., Jain, R.M., Prasanth, S., Venugopalan, R.B. (2013). "Investigation on infrastructural damages by rainfall-induced landslides during November 2009 in Nilgiris, India." *Nat Hazards* 65(3):1535–1557
- [10]. Chen, X.L., Liu, C.G., Chang, Z.F., Zhou, Q. (2016). "The relationship between the slope angle and the landslide size derived from limit equilibrium simulations." *Geomorphology* 253:547–550

- [11].Conte, E., Troncone, A. (2012). “A method for the analysis of soil slips triggered by rainfall.” *Geotechnique* 62(3):187–192
- [12].Crosta G, Frattini P (2008) “Rainfall-induced landslides and debris flows.” *Hydrol Process* 22(4):473–477
- [13].Dahal RK, Hasegawa S, Yamanaka M, Dhakal S, Bhandary NP, Yatabe R (2009) “Comparative analysis of contributing parameters for rainfall-triggered landslides in the Lesser Himalaya of Nepal.” *Environ Geology* 58(3):567–586
- [14].Dahal, R. K; Hasegawa, S; Nonomura,A ; Yamanaka,M ; Masuda,T; Nishino,K (2008) “Failure characteristics of rainfall-induced shallow landslides in granitic terrains of Shikoku Island of Japan,” *Environ Geol* (2009) 56:1295–1310
- [15].Floris M, Bozzano F (2008) “Evaluation of landslide reactivation: a modified rainfall threshold model based on historical records of rainfall and landslides.” *Geomorphology* 94(1):40–57
- [16].Fourie AB, Rowe D, Blight GE (1999) “The effect of infiltration on the stability of the slopes of a dry ash dumps.” *Geotechnique* 49(1):1–13
- [17].Frattini P, Crosta GB (2013) “The role of material properties and landscape morphology on landslide size distributions.” *Earth Planet Sci Lett* 361:310–319
- [18].Ghiassian, H.; Ghareh, S. (2008) “Stability of sandy slopes under seepage conditions.” *Landslides*, Volume 5:397_406.
- [19].Glade T, Crozier M, Smith P (2000) “Applying probability determination to refine landslide-triggering rainfall thresholds using an empirical Antecedent daily rainfall model.” *Pure Appl Geophys* 157:1059–1079
- [20].Godt JW, Baum RL, Chleborad AF (2006) “Rainfall characteristics for shallow landsliding in Seattle, Washington, USA.” *Earth Surf Process Landf* 31:97–110
- [21].Guzzetti F, Peruccacci S, Rossi M, Stark CP (2007) “Rainfall thresholds for the initiation of landslides in central and southern Europe.” *Meteorog Atmos Phys* 98:239–268
- [22].Harp, E.L.; Wells, W.G.; Sarmiento, J. (1990) “Pore pressure response during failure in soils.” *Geological Society of America Bulletin*, Volume 102:428_438.
- [23].Himachal Pradesh State Disaster Management Authority-HPSDMA (2012) Activity Report (2007–2011). Government of Himachal Pradesh, Department of Revenue (Disaster Management Cell). www.hpsdma.nic.in

- [24].Iverson RM (2000) “Landslide triggering by rain infiltration.” *Water Resour Res* 36(7):1897–1910
- [25].Iverson, R.; Reid, M.; R.G., L. (1997) “Debris-Flow Mobilization from Landslides.” *Annu. Rev. Earth Planet. Sci.*, Volume 25:85_138.
- [26].Iverson, R.M.; Major, J.J. (1986) “Groundwater Seepage Vectors and the Potential for Hillslope Failure and Debris Flow Mobilization.” *Water Resources Research*, Volume 22(11):1543_ 1548.
- [27].Joshi S, Kumar K, Joshi V, Pande B (2014) “Rainfall variability and indices of extreme rainfall analysis and perception study for two stations over Central Himalaya, India.” *Nat Hazards* 72(2):361–374.
- [28].Kanungo DP, Sharma S (2014) “Rainfall thresholds for prediction of shallow landslides around Chamoli- Joshimath region, Garhwal Himalayas, India.” *Landslides* 11(4):629–638
- [29].Li Chi, Yao De, Wang Zhong, Liu Chuancheng, Wuliji Nashun, Yang Liu, Li Lin, Amini Farshad (2016) “Model test on rainfall-induced loess–mudstone interfacial landslides in Qingshuihe, China.” *Environ Earth Sci* (2016) 75:835
- [30].Lourenco, S.D.; Sassa, K.; Fukuoka, H. (2006) “Failure process and hydrologic response of a two layer physical model: Implications for rainfall-induced landslides.” *Geomorphology*, Volume 73:115_130.
- [31].Luo, Y; He,S;Chen,F; Li,X; He.J(2015) “A physical model considered the effect of overland water flow on rainfall-induced shallow landslides.” *Geoenvironmental Disasters* (2015) 2:8
- [32].Mahanta B, Singh HO, Singh PK, Kainthola A, Singh TN (2016) “Stability analysis of potential failure zones along NH-305, India.” *Nat Hazards* 83(3):1341–1357
- [33].Mikos, M.; Cetina, M.; Brilly, M. (2004) “Hydrologic conditions responsible for triggering the Stoze landslide, Slovenia.” *Engineering Geology*, Volume 73(3-4):193_213.
- [34].Okura Y, Kitahara H, Ochiai H et al (2002) “Landslide fluidization process by flume experiments.” *Eng Geol* 66(1):65–78.
- [35].Pandey AK, Sachan HK, VirDI NS (2004) “Exhumation history of a shear zone constrained by microstructural and fluid inclusion techniques: an example from the Satluj valley, NW Himalaya, India.” *J Asian Earth Sci* 23(3):391–406.

- [36]. Ramakrishnan D, Singh TN, Verma AK, Gulati A, Tiwari KC (2013) “Soft computing and GIS for landslide susceptibility assessment in Tawaghat area, Kumaon Himalaya, India.” *Nat Hazards* 65(1):315–330
- [37]. Rogers, N.; Selby, M. (1980) “Mechanisms of shallow translational landsliding during summer rainstorm: North Island, New Zealand.” *Geografska Annaler*, Volume 62 A((1 2)):11_21.
- [38]. Sanchi's J, Boovi D, Al-Harbi Naif A, Silva LF, Farre' M, Barcelo' D (2013) “Quantitative trace analysis of fullerenes in river sediment from Spain and soils from Saudi Arabia.” *Anal Bioanal Chem (Print)* 405:5915–5923
- [39]. Sarkar K, Singh AK, Niyogi A, Behera PK, Verma AK, Singh TN (2016) “The assessment of slope stability along NH-22 in Rampur-Jhakri Area, Himachal Pradesh.” *J Geol Soc India* 88(3):387–393
- [40]. Sarkar K, Singh TN, Verma AK (2010) “A numerical simulation of landslide-prone slope in Himalayan region—a case study.” *Arab J Geosci* 5(1):73–81
- [41]. Sarkar S, Samanta M (2017) “Stability analysis and remedial measures of a landslip at Keifang, Mizoram—a case study.” *J Geol Soc India* 89(6):697–704
- [42]. Sengupta A, Gupta S, Anbarasu K (2010) “Rainfall thresholds for the initiation of landslide at Lanta Khola in north Sikkim, India.” *Nat Hazards* 52(1):31–42
- [43]. Senthilkumar, V; Chandrasekaran,s,s; Maji, V.B(2017) “Geotechnical characterization and analysis of rainfall—induced 2009 landslide at Marappalam area of Nilgiris district, Tamil Nadu state, India.” *Landslides* (2017) 14:1803–1814
- [44]. Singh, A.K., Kundu, J., Sarkar, K. (2017) “Stability analysis of a recurring soil slope failure along NH-5, Himachal Himalaya, India.”
- [45]. Skempton AW (1985) “Residual Strength of clays in landslide, folded strata, and the laboratory.” *Geotech Lond* 1(38):3–18.
- [46]. Take WA (2004) “Bolton evaluation of landslide triggering mechanisms in model fill slopes.” *Landslides* 1(3):173–184.
- [47]. Terzaghi K (1950) “Mechanism of landslides.” In: *Berkey geological society of America*, pp 83–123
- [48]. Yang H, Wang F, Vilimek V, Araiba K, Asano S (2015) “Investigation of rainfall-induced shallow landslides on the northeastern rim of Aso caldera, Japan, in July 2012.” *Geoenvironmental Disasters* (2015) 2:20